МІНІСТЕРСТВО ОСВІТИ І НАУКИ УКРАЇНИ
ДЕРЖАВНИЙ УНІВЕРСИТЕТ «КИЇВСЬКИЙ АВІАЦІЙНИЙ ІНСТИТУТ»
ФАКУЛЬТЕТ АЕРОНАВІГАЦІЇ, ЕЛЕКТРОНІКИ ТА ТЕЛЕКОМУНІКАЦІЙ
КАФЕДРА АВІОНІКИ ТА СИСТЕМ УПРАВЛІННЯ

ДОПУСТИТИ ДО ЗАХИСТУ
Завідувач кафедри
_____О. М. ТАЧИНІНА
«_____» _____2025 р.

КВАЛІФІКАЦІЙНА РОБОТА

(ПОЯСНЮВАЛЬНА ЗАПИСКА)

ВИПУСКНИКА ОСВІТНЬОГО СТУПЕНЯ
«БАКАЛАВР»

Тема: «**Трьох-режимний вібраційний гіроскоп**»

Виконавець: студент групи _____Ярослав ТАРНАВСЬКИЙ

Керівник: професор _____Валерій ЧІКОВАНІ

Нормоконтролер:_____ Микола ДИВНИЧ

Київ 2025

MINISTRY OF EDUCATION AND SCIENCE OF UKRAINE
STATE UNIVERSITY “KYIV AVIATION INSTITUTE”
FACULTY OF AIR NAVIGATION, ELECTRONICS AND TELECOMMUNICATIONS
AVIONICS AND CONTROL SYSTEMS DEPARTMENT

APPROVED FOR DEFENCE
Head of the Department
_____ O. M. TACHYNINA
“____” _____ 2025

QUALIFICATION PAPER

(EXPLANATORY NOTE)

FOR THE ACADEMIC DEGREE OF BACHELOR

Title: **“Triple-mode vibratory gyroscope**”

Submitted by:
student of group Ба-151-21-2-СУ _____ Yaroslav TARNAVSKYI

Supervisor: professor _____ Valerii CHIKOVANI

Standards inspector_____ Mykola DYVNYCH

Kyiv 2025

ДЕРЖАВНИЙ УНІВЕРСИТЕТ «КИЇВСЬКИЙ АВІАЦІЙНИЙ ІНСТИТУТ»

Факультет аеронавігації, електроніки та телекомунікацій

Кафедра авіоніки та систем управління

Спеціальність: 151 «Автоматизація та комп'ютерно-інтегровані технології»

ЗАТВЕРДЖУЮ

Завідувач кафедри

_____ О. М. ТАЧИНІНА

«_____»_____2025 р.

ЗАВДАННЯ

на виконання кваліфікаційної роботи

Тарнавського Ярослава Михайловича

1. Тема кваліфікаційної роботи «Трьох-режимний вібраційний гіроскоп» затверджена наказом ректора від “20” 03 2025 р. №429/Ст

2. Термін виконання роботи: з 19.05.2025 р. по 14.06.2025 р.

3. Вихідні дані роботи: Блок-схеми трьох режимів роботи вібраційного гіроскопа та її Симулінк моделі.

4. Зміст пояснювальної записки: Режим датчика кутової швидкості, Режим інтегруючого гіроскопа, Режим диференційного гіроскопа, Результати моделювання трьох режимного гіроскопа, висновки, література.

5. Перелік обов’язкового ілюстративного матеріалу: блок схеми, Симулінк модель, презентація у Power point.

6. Календарний план-графік

№ пор.	Завдання	Термін виконання	Відмітка про виконання
1	Отримання теми дипломної роботи	05.05.2025	Виконано
2	Написання першого розділу роботи	07.05.2025	Виконано
3	Написання другого розділу роботи	27.05.2025	Виконано
4	Подача керівнику першого та другого розділів на перевірку	28.05.2025	Виконано
5	Написання третього та четвертого розділів роботи	5.06.2025	Виконано
6	Подача керівнику матеріалів диплома на перевірку	9.06.2025	Виконано
7	Оформлення дипломної роботи	12.06.2025	Виконано
8	Підготовка презентації та доповіді	14.06.2025	Виконано

7. Дата видачі завдання: «05» 05 2025 р.

Керівник кваліфікаційної роботи_____ Валерій ЧІКОВАНІ
(підпис керівника)

Завдання прийняв до виконання_____Ярослав ТАРНАВСЬКИЙ
(підпис випускника)

STATE UNIVERSITY “KYIV AVIATION INSTITUTE”

Faculty of Air Navigation, Electronics and Telecommunications

Avionics and Control Systems Department

Specialty: 151 “Automation and Computer-integrated Technologies”

APPROVED BY

Head of the Department

_____ O. M. TACHYNINA

“_____”_____2025

Qualification Paper Assignment for Graduate Student

Tarnavskyi Yaroslav Mychailovych

1. The qualification paper title “Triple-mode vibratory gyroscope” was approved by the Rector’s order of “20” 03 2025 p. No.429/Ст.

2. The work was carried out between: 19.05.2025 to 14.06.2025

3. Initial data for the work: Block diagrams of the three operating modes of a vibratory gyroscope and their Simulink models

4. The content of the explanatory note: The rate-mode vibratory gyroscope, The rate-integrating mode gyroscope, The differential mode vibratory gyroscope, The triple-mode vibratory gyroscope and simulation results, Conclusions, References

5. The list of mandatory illustrations: Block diagrams, Simulink model, presentation in Power point.

6. Timetable

№	Assignment	Dates of completion	Completion mark
1	Obtaining a thesis topic	05.05.2025	Done
2	Writing the first section of the work	07.05.2025	Done
3	Writing the second section of the work	27.05.2025	Done
4	Submitting the first and second sections to the supervisor for review	28.05.2025	Done
5	Writing the third and fourth sections of the work	5.06.2025	Done
6	Submitting diploma materials to the supervisor for review	9.06.2025	Done
7	Completion of the diploma	12.06.2025	Done
8	Preparation of the presentation and the report	14.06.2025	Done

7. Assignment issue date: “05” 05 2025

Qualification paper supervisor _____ Valerii CHIKOVANI
(the supervisor’s signature)

Issued task accepted _____ Yaroslav TARNAVSKIY
(the graduate student’s signature)

РЕФЕРАТ

Пояснювальна записка до кваліфікаційної роботи "Трьох-режимний вібраційний гіроскоп", містить 85 сторінок, 6 таблиць, 13 джерел.

Актуальність теми Трьох-режимний вібраційний гіроскоп — це інноваційна концепція, яка об’єднує три функціональні режими в одному пристрої з можливістю автоматичного перемикання між ними залежно від умов роботи. Такий підхід дозволяє істотно розширити функціональні можливості гіроскопа, підвищити його точність, стабільність і адаптованість до умов навколишнього середовища і руху.

Об'єктом дослідження є вібраційний гіроскоп, включаючи мікро-електро-механічний гіроскоп.

Предметом дослідження є режими роботи вібраційного гіроскопа.

Метою роботи є аналіз похибок кожного режиму роботи вібраційного гіроскопа та їх переваг та недоліків за допомогою комп’ютерного моделювання та методів аналізу даних моделювання.

Методи дослідження включають моделювання в Matlab Simulink, метод найменших квадратів для вилучення похибок, аналіз даних і методи апроксимації складних функцій.

Ключові слова: ІНТЕГРУЮЧИЙ РЕЖИМ, МІКРО-ЕЛЕКТРО-МЕХАНІЧНИЙ ГІРОСКОП, МОДЕЛЮВАННЯ, АНАЛІЗ ДАНИХ.

ABSTRACT

Explanatory note for the qualification paper "Triple-mode vibratory gyroscope" includes: 85 pages, 6 tables, 13 references.

The relevance of the topic A triple-mode vibratory gyroscope is an innovative concept that integrates three functional modes within a single device with the ability to automatically switch between them depending on the operating conditions. This approach allows for a significant expansion of the gyroscope's functionality, improving its accuracy, stability and adaptability to invironmental and motion condition.

The object of the study is the vibratory gyroscope including the micro-electro-mechanical gyroscope.

The subject of the research is vibratory gyroscope modes of operation

The aim of the work is an analysis of the errors of each mode of operation of the vibration gyroscope and their advantages and disadvantages using computer modeling and simulation data analysis methods

Research methods include simulation in Matlab Simulink, least squares method for error extraction, data analysis, and complex function approximation methods.

Key words: INTEGRATING MODE, MICRO-ELECTRO-MECHANICAL GYROSCOPE, SIMULATION, DATA ANALYSIS.

Contents

INTRODUCTION

In today's world of dynamic development of engineering and technology, especially in the field of navigation systems, gyroscopic devices play a key role. They are used to determine the angular velocity, position and orientation of objects in space, which is especially important in aviation, marine navigation, rocketry, robotics, mobile devices and other high-tech industries. A special place among these devices is occupied by vibratory gyroscopes, which have become extremely popular due to their compactness, reliability, low power consumption and the possibility of implementation on a microscale (in the form of MEMS devices).

Vibratory gyroscopes are based on the Coriolis effect, which occurs when an oscillating mass interacts with rotation. They are divided into several main types according to their operating principle: rate-mode (angular rate sensor mode), rate-integrating mode, and differential mode. Each of these modes has its own advantages and limitations, which necessitates an integrated approach to designing devices that can operate effectively in different conditions.

A three-mode vibratory gyroscope is an innovative concept that integrates three functional modes within a single device with the ability to automatically switch between them depending on the operating conditions. This approach allows for a significant expansion of the gyroscope's functionality, improving its accuracy, stability and adaptability. In the future, this may enable the creation of universal navigation systems for a wide range of applications, from autonomous vehicles to spacecraft.

The relevance of the research topic is that most modern systems use gyroscopes with one fixed mode of operation, which limits the flexibility of their application. The development of a gyroscope capable of operating in three modes with the possibility of modelling and verification in the Simulink environment is an important step towards creating more intelligent, versatile and resistant to external disturbances sensor systems.

Purpose of the work:

Development of a structural concept, mathematical model and implementation of a simulation model of a three-mode vibratory gyroscope in Simulink, with further analysis of operation in each mode and automatic switching between them.

Objectives:

- To analyse the principles of operation of vibratory gyroscopes in the modes of rate-mode (angular rate sensor mode), rate-integrating mode and differential mode.

- To study the main types of errors and factors affecting the accuracy of vibratory gyroscopes.

- Create structural block diagrams of control systems for each mode.

- Justify the feasibility of integrating the modes in a single device.

- Develop a simulation model of a three-mode vibratory gyroscope in the Simulink environment.

- Simulate the operation of the device, analyse the results and check the possibility of switching between modes.

Object of study:

The process of measuring angular velocities and position of objects using a vibratory gyroscope.

Subject of research

Methods of building a multi-mode vibratory gyroscope system, control principles and software implementation in Simulink.

Research methods

To achieve this goal, the following methods are used:

- methods of system analysis for building structural schemes;

- theoretical methods for studying oscillatory systems;

- mathematical modelling of gyroscope dynamics;

- simulation modelling in MATLAB/Simulink;

- comparative analysis of operating modes.

Scientific novelty

For the first time, the concept of a three-mode vibratory gyroscope with automatic switching between modes of operation under conditions modelled in the Simulink environment was implemented at the level of an undergraduate study. This approach allows to increase the efficiency of sensor systems in dynamically changing conditions.

Practical relevance

The developed model can be used as a basis for creating software, microcontroller algorithms or real-time systems in the field of robotics, aviation, and autonomous vehicles. The modelling results can be used in the educational process when teaching courses on mechatronics, sensors and automatic control.

Structure of the thesis

The thesis consists of four chapters. The first three chapters are devoted to the theoretical analysis of the vibratory gyroscope operating modes. The fourth chapter contains the practical part, i.e., the construction of the model in Simulink and the analysis of its operation. The paper is completed with conclusions, references and appendices.

SECTION 1. The rate-mode vibratory gyroscope

1.1. Principle of operation of the rate-mode vibratory gyroscope

Vibratory gyroscopes are inertial sensors that measure the angular velocity of the object to which they are attached using the Coriolis effect. In the Rate Mode, the vibratory gyroscope operates as a detector of instantaneous angular velocity in one or more axes.

The principle of operation of an oscillatory gyroscope is based on the property of a mass that performs oscillatory movements to be affected by the Karyolis force during the rotation of the system. When a body of mass m moves with velocity v in a system rotating with angular velocity ω, it is subject to the Coriolis force, which is defined by the formula:

$$Fc = -2m(\omega \times v) \quad (1.1)$$

This force does not generate work, but changes the trajectory of the mass, which allows the rotation to be detected. In an oscillating gyroscope, the force causes the moving element to shift from its original trajectory, which is detected by a sensor.

A typical structure of a vibratory gyroscope consists of:

- a driving unit (drive mode) that produces the main mass oscillations in one plane;
- a sensing unit (sense mode) that detects the deflection caused by rotation in a perpendicular plane;
- a mechanical resonator (e.g., a double fork, spring frame, or ring structure);
- an electronic amplifier and filter for signal processing;
- an output converter for converting the analogue signal to digital

The most common example is a tuning fork gyroscope, which consists of two identical masses oscillating in opposite directions (similar to the teeth of a tuning fork). When the device is not rotating, the trajectory of the masses is symmetrical, and the Coriolis forces are mutually compensated. However, when rotating about an axis perpendicular to the plane of oscillation, deviations appear in the direction perpendicular to both the rotation vector and the direction of oscillation. These deviations are detected by sensors.

Rate mode CVG

CVGs fall into two classes, depending on the nature of the two vibratory modes involved. In the first class, the modes are different. An example of this class is the bar and tuning fork gyros, in which the mode driven is the ordinary vibratory mode of the fork – primary mode, while the second or readout mode is the torsional oscillation of the fork about its axis of symmetry – secondary mode. The primary and secondary modes of bar and tuning fork gyros are depicted in fig.1.

In the second class, the two modes are identical, being two orthogonal modes (modes of the same natural frequency) of an axisymmetric elastic body. Examples are the vibrating cylindrical and hemispherical shells and ring, as depicted in fig.2, and in fact any shell obtained as a body of rotation.

The operation of a Coriolis vibratory gyroscope is based on sensitivity of elastic resonant structures to inertial rotation.

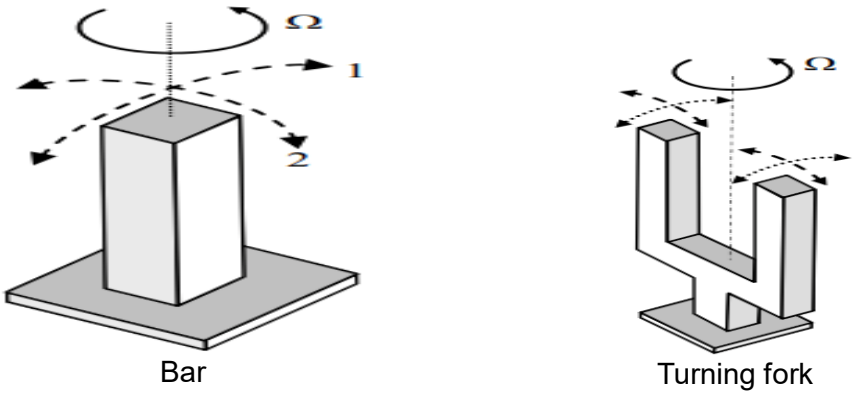

Fig. 1.1 – Resonators for the first class CVG

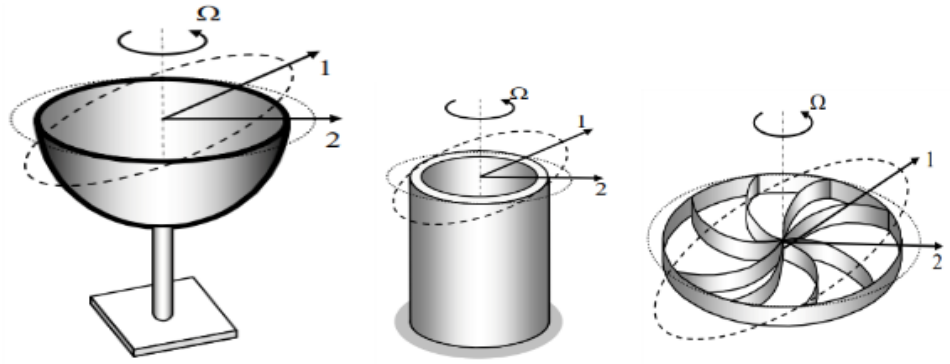

Hemi-spherical shell Cylinder shell Ring

Fig. 1.2 – Resonators for the second class CVG

One of the most important parameters of resonators is quality factor (Q-factor), which depends on properties of a material from which the resonator is manufactured, and also on degree of an asymmetry of its shape etc. and is determined as:

$$Q = \frac{\omega_r \tau}{2} = \pi f_r \tau \qquad (1.2)$$

where ω_r and f_r are circular and cyclic resonant frequency of a resonator, τ is a time of free oscillations amplitude damping *e* times.

In this paper we will focus on the second class CVG. Ring-type resonators shown in Fig.1.2. use the second mode of vibration to measure angular rate, because it has maximum sensitivity to rotation.

Fig.1.3. shows the standing wave on the second resonant mode of the ring-type resonator which is characterized by 4 antinodes (maximum vibration amplitude) and 4 nodes (minimum vibration amplitude) located along circumferential coordinate under angles of 45 deg.

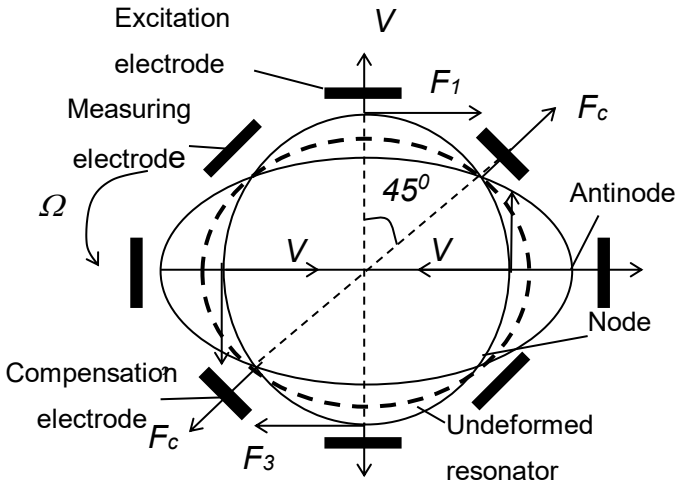

Fig.1.3 – Standing wave in ring-type resonator

Under resonator rotation with angular rate Ω, there arise Coriolis forces F_1, F_2, F_3, F_4 (fig.1.3), which generate secondary (Coriolis) mode of vibration in the direction of resultant force F_c.

Resultant Coriolis force is proportional to angular rate, Ω:

$$ {}^{I}F_c = 2m\left[{}^{I}\Omega \times {}^{I} V\right] \qquad (1.3)$$

where V is a linear velocity of radial motion in process of vibration; m is an effective vibrating mass.

Thus, vibration amplitude generated by Coriolis force is proportional to angular rate Ω. Secondary (Coriolis) mode amplitude is measured by the electrode located at the node of the primary standing wave and with the aid of feedback control system is damped by applying compensation signal on the other node. Feedback control signal that compensates secondary mode of vibration is proportional to angular rate. Standing

wave control system of the rate gyro is depicted in fig.4

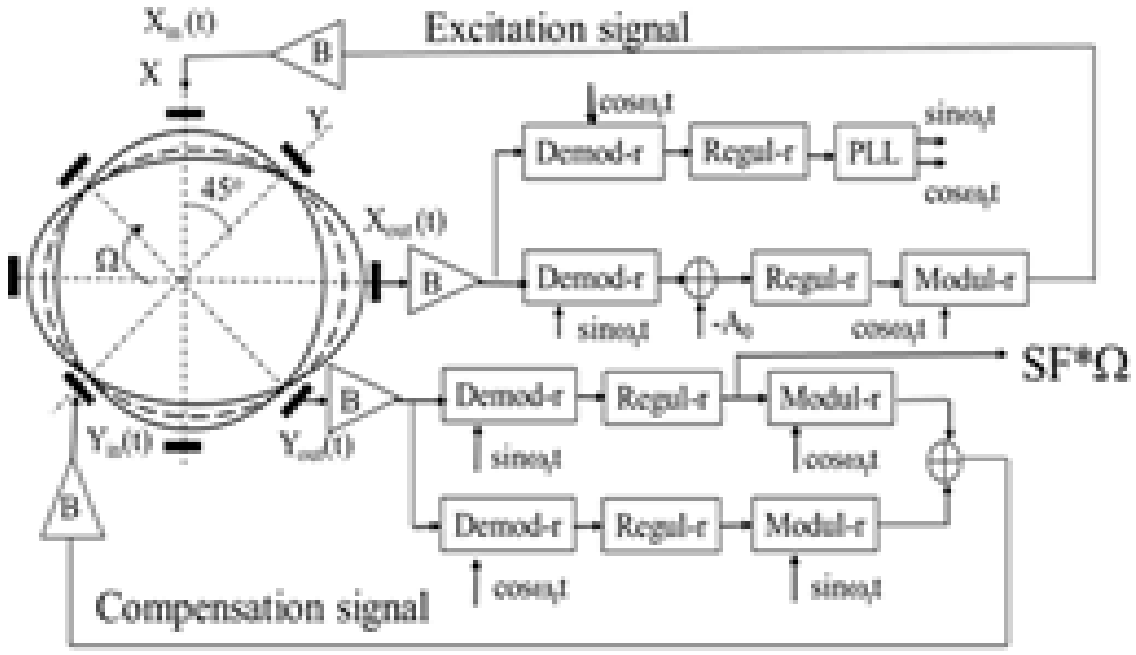

Fig.1.4 – Rate CVG control system block

Diametrically opposite electrodes are connected between each other. As a result sensor has two input signals (Xin, Yin) and two output signals (Xout, Yout) (see fig.1.4). It means that sensor can be considered as two-input-two-output plant. Vibration excitation is provided by supplying periodical signal to the Xin electrode at the resonant frequency. Response is picked off from the Xout electrode and it is used to sustain vibration and to track for changing of resonant frequency. Secondary mode amplitude is picked off from the Yout electrode located at the nodal point of the primary wave and with the help of negative feedback signal is suppressed by supplying opposite phase signal to the Yin electrode located at the other nodal point of the primary

wave. Thus, feedback signal amplitude that compensates for the node vibration is proportional to angular rate Ω.

As has been shown in fig.1.4, after demodulation of signal from Yout electrode using reference signal sinωrt, regulator generates compensation signal which is proportional to angular rate Ω. Coefficient of proportionality called scale factor (SF) and bias B as an error component can be determined as:

$$\Omega = \frac{1}{SF}\,\mathrm{demod}\{Y_{out}\}|_{\sin\omega_r t} + B \tag{1.4}$$

$$SF = 2k\omega_r A_0; \quad B = \frac{1}{2k}\,\Delta\left(\frac{1}{\tau}\right)\sin\theta_\tau \tag{1.5}$$

where A_0 is vibration amplitude, k is Brian coefficient determined by mode of vibration and resonator geometry, $\Delta(1/\tau)$ is a measure of resonator material non-homogeneity, θ_τ is a direction of maximum damping of resonator free oscillations. $\Delta(1/\tau)$ and θ_τ reduce to minimum by resonator mass-balancing procedure.

Suppose that the mass m = 0.01 kg, the excited oscillation velocity v = 0.2 m/s, and the angular velocity of rotation ω = 10 rad/s. Then the Coriolis force will be:

$$Fc = 2 \times 0.01 \times 10 \times 0.2 = 0.04 \text{ H}$$

This force produces a displacement in the sensor direction, which is processed as an output signal proportional to ω. Taking into account the calibration and the scaling factor Ks, which in industrial gyroscopes can be 0.5-10 mV/(rad/s), we obtain the output voltage $U_{out} = K_s \times \omega$.

For K_s = 5 mV/(rad/s) at ω = 10 rad/s, we obtain:

$U_{out} = 5 \times 10 = 50$ mV

Mode analysis

Advantages of a vibratory gyroscope in rate-mode (angular rate sensor mode):

- High sensitivity to changes in angular velocity;
- Fast response to rotation - low inertia;

- Relatively simple signal processing algorithm;

- Well suited for stabilisation and orientation systems.

Disadvantages:

- Errors due to temperature instability of the material;

- Zero shift (biasdrift), especially in MEMS gyroscopes;

- Limited accuracy when integrating to obtain a position (due to error accumulation);

- Need for high-precision calibration at small rotation angles.

Applications

The rate-mode (angular rate sensor mode) is used in many devices:

- Smartphones and tablets (e.g. for image stabilisation or gesture recognition);

- Camera stabilisation systems (gimbalsystems);

- Automotive safety systems (ESC, ABS);

- Unmanned aerial vehicles (drones, UAVs);

- Robotics and game controllers.

The principle of operation of the vibratory gyroscope in the rate-mode (angular rate sensor mode) is based on the direct relationship between the deflection of the mass due to the action of the Coriolis force and the angular velocity of rotation. This mode remains one of the most versatile and widespread due to its ease of implementation, speed and relative reliability. At the same time, its limitations necessitate the search for ways to combine it with other modes (integration, differentiation), which became the basis for the development of a three-mode vibratory gyroscope, as discussed in the following sections.

1.2. Block diagram of the control system and main errors of the gyroscope

The control system of a vibratory gyroscope in the rate-mode (angular rate sensor mode) is critical to ensure the accuracy, stability, and speed of the device. The main purpose of the control system is to maintain stable oscillations of the excited element (active oscillation), as well as to accurately read the signal resulting from the action of the Coriolis force in the sensor channel. To achieve this goal, special electronic systems are developed that provide feedback, error compensation and signal filtering.

At the top of the circuit, there is an excitation generator (DriveOscillator) that generates a stable harmonic signal with a frequency close to the natural frequency of the elastic system. This signal is fed into the DriveMechanism, a mechanical or electrostatic subsystem that causes the gyro mass to oscillate in the X-plane. The excitation frequency is usually resonant (e.g. 2 kHz), which allows for maximum amplitude with minimum power consumption.

Oscillations of the mass in the X-plane when the device is rotated around the Z-axis cause the emergence of the Coriolis force acting in the perpendicular direction - along the Y-axis. This force causes a displacement of the mass in the sensor direction, which is proportional to the angular velocity. The displacement is detected by a sensor system (DisplacementDetector), which generates a corresponding electrical signal.

This signal is then processed in an analogue amplifier (AnalogAmplifier), where its amplitude is increased to a level suitable for digital processing. The signal is then sent to an analogue-to-digital converter (ADC), where it is converted into a digital code.

The digital data is then sent to the Digital Processing Unit. This is where filtering, error compensation and the calculation of angular velocity or angle of rotation take place. Filters (e.g. digital low-pass or adaptive Kalman) suppress noise and interference components. This is where the scaling is done to match the sensitivity of the sensor, for example, 6 mV/rad/s.

In the central part of the circuit, there is a phase locked loop (PLL) - a phase-locked oscillator that synchronises the excitation frequency with the actual oscillation frequency. This is necessary to maintain resonance in the face of temperature drift or

material aging. For example, when the temperature changes by 20 °C, the frequency can change by 1-2 Hz, which requires constant correction.

The key part of the scheme is the Error Compensation Module. The main sources of errors that are taken into account are:

1. Temperature drift of the frequency - due to changes in the stiffness and geometry of the elastic system. It is compensated by thermal sensors and mathematical models (correction tables).

2. External vibrations - affect the movement of the mass similarly to the Coriolis force, therefore causing parasitic signals. Compensation is performed by accelerometers or digital filtering.

3. Electronics noise - high-frequency pickups, power supply instability. Compensated by hardware stabilisation, filters and shielding.

4. Frequency mismatch between modes - disturbance of the sensor axis resonance mode. Active frequency matching is used by means of electrostatic adjustment or change of the drive signal.

The processing output signal is fed to the Output Interface, which is transmitted to external systems via UART, SPI, I2C or analogue interfaces.

Thus, the block diagram shows the full cycle of the gyroscope - from oscillation generation and maintenance to processing and error compensation, providing accurate angular velocity measurement. It is the basic structure used in most modern MEMS gyroscopes, including three-mode systems that operate in both rate-mode and rate-integrating or differential modes.

1. Exciter (DriveLoop) - generates and maintains oscillations of the working mass at the resonant frequency. As a rule, this oscillation occurs along the X-axis.

2. Feedback loop (PhaseLockedLoop, PLL) - maintains the phase synchronisation of the excitation signal with the resonator's own oscillations by adjusting the oscillator frequency.

3. Sensor channel (SenseLoop) - measures the signal caused by the Coriolis force (Y or Z axis), converting the mechanical deflection into an electrical voltage.

4. Compensation loop (ForceRebalanceLoop) - performs an inverse action on the mass to maintain its stable position, generating a signal proportional to the angular velocity.

5. Filter (Low-pass / Band-passFilter) - filters noise and high-frequency signal distortion.

6. ADC/DAC and microcontroller - perform digital signal processing, compensation of temperature and mechanical errors, scaling and transmission of information to a higher level of the system.

In many industrial implementations, PID controllers are used to maintain a stable amplitude-phase oscillation mode, as well as digital adaptive processing algorithms (e.g., Kalman filter or digital estimation methods).

Let's assume that the resonator oscillation frequency is f_d = 18 kHz, the excitation amplitude is A = 10 μm, and the mass of the working element is m = 0.015 g. In the case of rotation with an angular velocity ω = 20 rad/s, a displacement in the perpendicular direction occurs under the action of the Coriolis force, which is recorded by the sensor system. If the scale factor of the system is Ks = 8 mV/(rad/s), the output voltage will be

$$U_{out} = Ks \cdot \omega = 8 \cdot 20 = 160mV \quad (1.6)$$

After filtering and analogue-to-digital conversion, this signal is fed into the digital control system.

The main sources of error in a vibratory gyroscope

Despite the high sensitivity and compact size of vibratory gyroscopes, their accuracy is limited by a number of internal and external errors. The main sources of errors include:

1. Zero shift (Bias Instability) is the most important error, which manifests itself as a random or temperature-dependent change in the zero signal level.

2. Noise Density - characterises random fluctuations of the measured signal.

3. Temperature instability - changes the mechanical properties of the resonator.

4. Parasitic oscillations (Quadrature Error) - caused by imperfect manufacturing of the structure.

5. Phase shifts and control delays - can lead to system instability.

6. Dynamic acceleration errors - transverse and longitudinal accelerations can modify the performance of the sensor channel.

Table 1.1 – Accuracy and error parameters of typical gyroscopes in the rate-mode (angular rate sensor mode)

Parameter	Domestic MEMC	Automotive class	Precision gyroscope
Zero offset (bias)	±20 °/hour	±3 °/hour	< 0.1 °/hour
Noise (noise density)	0.1 °/√Hz	0.02 °/√Hz	0.005 °/√Hz
Zero temperature dependence	200 ppm/°C	50 ppm/°C	< 10ppm/°C
Excitation frequency	3–30 kHz	10–20 kHz	20–40 kHz

The control system of an vibratory gyroscope in the rate-mode (angular rate sensor mode) is a complex set of hardware and software solutions that help maintain the stability and accuracy of the measurement. The main errors of the system are related to thermal stability, noise and displacements, which is especially critical when using the gyroscope in autonomous navigation systems. It is these errors that necessitate in-depth modelling and development of new structures, including three-mode vibratory gyroscopes with the ability to automatically adapt to environmental changes, which will be discussed in further sections of this paper.

1.3. Types of vibratory gyroscopes: traditional and MEMS (tuning fork, ring, hemispherical, etc.)

Vibratory gyroscopes have a large number of design implementations that differ in the shape of the resonator, the principle of detecting the Coriolis force, and the manufacturing technology. In general, vibratory gyroscopes are divided into traditional macro-sized ones (placed in larger devices and having complex mechanical parts) and MEMS gyroscopes (Micro-Electro-Mechanical Systems), which are implemented on silicon wafers in the form of microscopic sensors. All of these types operate on the same physical principle - fixation of the Coriolis force that occurs when an oscillating body rotates.

1. Tuning Fork Gyroscope

This type of gyroscope uses two symmetrical masses that oscillate in opposite directions, similar to a tuning fork. During rotation, the Coriolis forces act on these masses in opposite directions, creating a measurable shear force. Cameron gyroscopes are among the most common due to their simple design, low cost, and compact size. They are usually made in the form of elastic frames or beams with masses at the ends.

Example parameters:

- Resonant frequency: 18-25 kHz
- Scale factor: 2-10 mV/(°/s)
- Accuracy: up to 1-2°/h in the best MEMS models
- Applications: smartphones, cameras, game controllers

2. Ring Gyroscope

This type of gyroscope uses a circular resonator - a ring or rim that vibrates with electrostatic or piezoelectric excitation. When rotating normal to the ring's plane, the vibration wave on the resonator shifts due to the Coriolis force. This design allows for higher sensitivity and stability due to the symmetry of the shape.

Example parameters:

- Vibration frequency: 20-80 kHz
- Noise: 0.02-0.05°/√Hz
- Temperature stability: up to 50 ppm/°C
- Output sensitivity: up to 20 mV/(°/s)
- Applications: automotive electronics, medical devices, unmanned aerial vehicles

3. Hemispherical Resonator Gyroscope (HRG)

One of the most precise types of vibratory gyroscopes, where the base is a thin-walled hemisphere, usually made of glass or ceramic, which carries out standing waves in the volumetric resonant mode. During rotation, the standing wave rotates within the resonator, which allows you to fix the angular velocity or even the full angle of rotation during integration.

: Example Parameters

– Resonant Frequency: 4–12 kHz

– Accuracy: < 0.01 °/h

– Operating Temperature Range: –50 to +85 °C

– Stability: < 1 ppm/year

– Applications: Aviation, Space, Launch Vehicles, Gyrostabilizers

Example: NASA's MarsInSight mission used a gyroscope with HRG with stability to 0.005 °/h over several months of operation.

4. Micro-Hemispherical Resonator Gyroscope (Micro-HRG)

This is a miniaturized version of the hemispherical vibratory gyroscope, manufactured using MEMS technology. It combines high sensitivity with compactness and suitability for mass production. However, due to the reduced size, the signal-to-noise ratio deteriorates and the influence of temperature factors increases.

Specifications:

– Frequency: up to 15 kHz

– Power consumption: < 5 mW

–Stability: up to 0.1 °/h

– Applications: autonomous systems, small drone navigation, military equip.

5. Other Geometric Types: Disk-shaped, Square, Linear

Among other configurations, there are disk-shaped gyroscopes, where vibrations occur in the plane of the disk; square resonators, which are easier to manufacture; U-shaped beams with good symmetry; as well as gyroscopes with linear or axial symmetry, used in specialized sensors.

Table 1.2 – Analytical Comparison

Gyroscope type	Sensitivity	Sizes	Stability	Applications
Forcing-type	Medium	Very small (MEMS)	Medium	Consumer electronics
Ring	High	Small	High	Automotive, medical equipment
Hemispherical (HRG)	Very high	Large	Very high	Space, aviation, missiles
Micro-HRG (MEMS)	High	Small	High	Navigation under constraints
Disk / square	Low–Medium	Small–medium	Medium	Specialized industrial devices

The diversity of vibratory gyroscope types provides flexibility in their applications — from basic sensors in smartphones to ultra-precise inertial systems in satellites. Tuning fork and ring gyroscopes are suitable for mass production due to their good cost-to-performance ratio, while HRGs offer the highest precision. The emergence of MEMS technology has opened new horizons for microscale implementations. Understanding the advantages and disadvantages of each type enables the correct selection of architecture when designing a three-mode vibratory gyroscope, where the properties of several types can be combined to enhance versatility and accuracy.

SECTION 2. The rate-integrating mode vibratory gyroscope

2.1. Principle of operation in the whole angle mode and control block diagram

The angular rate integration mode in a vibratory gyroscope, also known as the Full Angle Mode, involves not only detecting the instantaneous angular velocity, but also integrating it over time to determine the total rotation angle. This is particularly important in autonomous navigation tasks, where orientation changes must be tracked without relying on external coordinate sources such as GPS.

In the classical mode, the gyroscope records the instantaneous angular velocity ω(t), but in the integration mode, it performs the operation:

$$\theta(t) = \int_0^t \omega(\tau) d\tau \quad (2.1)$$

Thus, the output signal is not the instantaneous angular velocity value, but the rotation angle from the initial point in time.

To implement this mode, it is essential to ensure high system stability, minimize bias drift, noise, and parasitic shifts, which accumulate during integration and can cause significant position errors within just a few seconds of operation.

Let us consider the following scenario:

- Initial angular velocity of the object: ω = 5 rad/s
- Integration time: t = 2 s

Then the total rotation angle will be:

$$\theta = \int_0^2 5\ dt = 10\,\text{rad} \approx 572.96^\circ \tag{2.2}$$

If the bias error is only 0.02 rad/s, then the error after 2 seconds will be:

$$\Delta\theta = 0.02 \times 2 = 0.04\,rad \approx 2.3^\circ \tag{2.3}$$

This highlights the importance of bias compensation during integration.

The full-angle mode requires significant modifications in the control structure of the gyroscope compared to the rate mode.

Below is the logical control structure:

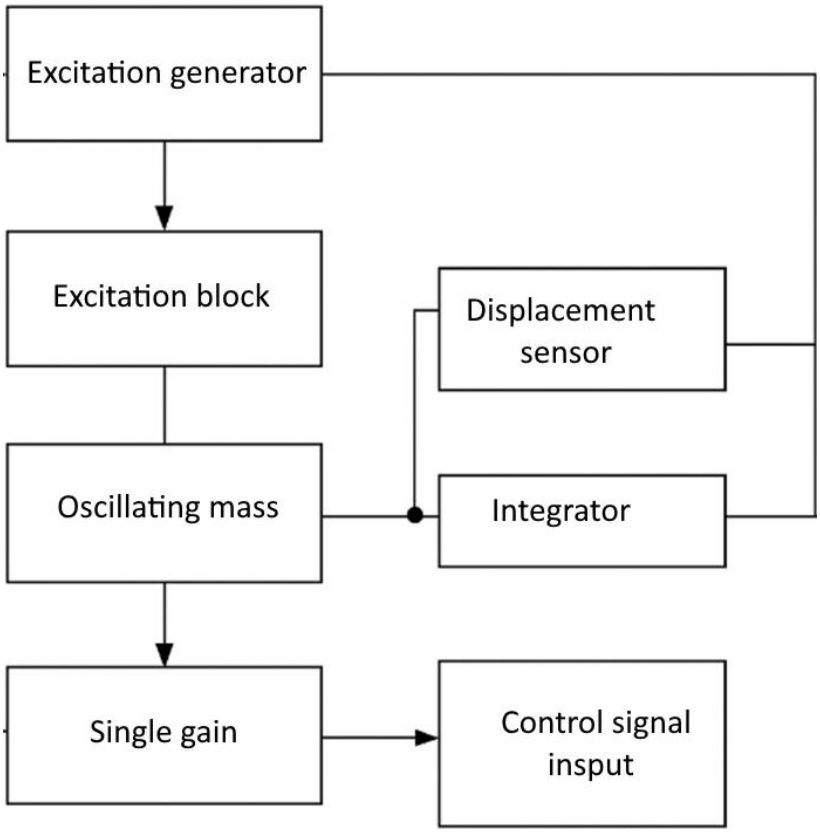

Fig. 2.1 – Block diagram of the control system for the vibratory gyroscope in rate-integrating mode

The system starts with a harmonic excitation generator, which creates a signal with a constant frequency, close to the resonant frequency of the vibrational system. This signal is fed to the active excitation mechanism (Drive Actuator), which sets the sensor mass into oscillatory motion along the X-axis. The amplitude and frequency of these oscillations are kept constant by a feedback stabilization system, which ensures that the motion remains in harmonic mode.

When the gyroscope rotates around the vertical axis (Z-axis), the mass oscillating in the X-plane experiences the Coriolis force, which is directed in the perpendicular plane (Y-axis). This force causes the displacement of the mass to increase in the sensor direction. The distinction of this mode is that the signal from the Coriolis force is not stabilized (as in the rate-mode), but integrated over time, allowing the determination of the total rotation angle.

The sensor displacement is recorded by a position sensor (Displacement Sensor), which detects the deviation of the mass in the Y-direction. The signal from the sensor is fed into an analog amplifier, where it is amplified and transmitted to the analog-to-digital conversion system (ADC).

The digital signal is processed in the digital processor (Digital Processor). In this block, not only noise filtering is carried out, but also the integration of angular velocity over time. Formally:

$$\theta(t) = \int_0^t \omega(\tau)\ d \tag{2.4}$$

θ(t) — rotation angle, ω(τ) — instantaneous angular velocity.

To implement this function in a microcontroller, numerical methods are used, specifically the rectangle method, trapezoidal method, or the Runge-Kutta method. The time resolution should be no less than 1–5 ms for precise integration in dynamic systems.

A key feature of the diagram is the presence of the zero bias correction block (ZeroBiasCorrection). Since even a small deviation in the zero level of speed (e.g., 0.05 °/s) during prolonged integration leads to a large angle error, this module constantly monitors drift and corrects the result. In high-precision systems, such a block is based on periodic zeroing, calibration on a stationary body, or digital averaging filtering.

The result of the system's operation is a signal proportional to the total rotation angle, which is sent to the data transmission interface (OutputInterface). This block can be implemented via UART/SPI or as an analog output (e.g., 0–5 V voltage for 0–360°).

Main advantages of the system:

- No need for an external integrator — everything is implemented in the digital processor.
- The possibility of use in navigation systems for tracking absolute position.
- Increased accuracy in short-term integrations.

Main issues and sources of errors:

- Zero bias error (drift),
- Noise accumulation during prolonged integration,
- Frequency mismatch between axes,
- Temperature instability.

In general, the block diagram visually demonstrates how the vibratory gyroscope transitions from rate-mode to rate-integrating mode — a more complex but strategically important mode for tasks where it is necessary to know not only the rotation speed but also the total change in orientation in space.

1. Filter — removes high-frequency fluctuations and noise that would otherwise turn into drift during integration.
2. Integrator — implemented digitally (for example, using the rectangle or trapezoidal method in MATLAB/Simulink).
3. Compensation Algorithm — periodically corrects the output based on reference data (e.g., from a magnetometer or by keeping an average bias value in the absence of rotation).

Table 2.1 – Analysis of the advantages and disadvantages of full-angle mode

Advantages	Disadvantages
Possibility of obtaining absolute position	Accumulation of error over time (drift)
Independence from external sources	Need for precise filtering and bias compensation
Relevant for inertial navigation	Significant increase in error at low signal-to-noise ratio
Suitable for orientation in a confined space	Need for more complex digital algorithms

The block diagram for the full-angle control mode demonstrates the sequence of functional steps that the signal undergoes in the vibratory gyroscope for integrating angular velocity and obtaining the absolute rotation angle. Below is a detailed explanation of each block in the diagram in logical order:

At the top part of the diagram is the vibration exciter (Drive), which is responsible for generating stable mechanical oscillations of the resonator in the specified plane (usually the X-axis). It creates the harmonic oscillatory environment necessary for the Coriolis effect to occur during rotation.

The next element is the phase-locked loop (PLL). Its function is to keep the resonant oscillation frequency at a constant level and ensure phase coherence between the excitation signal and the system's own mechanical oscillations. This ensures stable operation of the gyroscope because even small phase shifts can cause errors in sensor measurement.

Next, the signal moves to the sensor channel (Sense Mode), which detects the displacement of the moving mass caused by the Coriolis force resulting from rotation. These displacements occur in a direction perpendicular to the main oscillation plane

and are proportional to angular velocity. Accordingly, the sensor converts this displacement into a varying electrical voltage.

The obtained analog signal enters the analog-to-digital conversion (ADC) block. Here, it is digitized at a specified sampling frequency and prepared for further digital processing in the microcontroller or DSP processor. At this stage, it is important to ensure high resolution and sampling frequency to minimize distortions.

The digital signal enters the digital filtering block, where high-frequency noise, parasitic components (such as quadratic errors), and temporal fluctuations are removed. Band-pass filters, Kalman filters, or digital smoothing filters based on window processing are usually used at this stage.

After filtering, the signal proceeds to the key element — the digital integration block. Here, numerical integration of the angular velocity signal $\omega(t)$ over time is performed to calculate the rotation angle $\theta(t)$. Algorithms such as the rectangular method, trapezoidal method, or higher-order methods are used. This block is highly sensitive to zero drift, so it may incorporate a mechanism for periodic correction using external sources (e.g., a magnetometer).

The system ends with an output block, where the calculated rotation $\theta(t)$ is either stored or transmitted as a digital or analog signal. This result can be used for navigation decisions, stabilization, or further processing in higher-level control systems.

Thus, this block diagram describes the complete signal processing cycle in the gyroscope in full-angle mode — from oscillation generation to obtaining the integrated result. The system requires high precision synchronization, filtering, and error compensation, as even small zero shifts can lead to serious error accumulation during integration. Therefore, implementing such an architecture requires both physical improvements in sensors and software optimization of filters, compensation mechanisms, and computational algorithms.

2.2. Phenomenon of periodic zero displacement: causes and influence on accuracy

One of the most critical factors that limit the accuracy of a vibratory gyroscope, especially in the speed integration (full-angle) mode, is the phenomenon of zero drift (Zero-rate Output, Bias Drift). This occurs when, even in the absence of actual rotation (i.e., $\omega = 0$), the gyroscope generates a small non-zero output signal, which, due to its inertial logic, is interpreted as pseudo-rotation. If such a signal is integrated over a prolonged period, error accumulation occurs, leading to a significant drift in the calculated rotation angle.

Causes of Periodic Zero Drift

Zero drift has both static and dynamic causes. The main sources of this drift include:

1. Thermal Instability – Changes in temperature affect the elastic properties of the resonator materials, the frequency of oscillations, and the electrical sensitivity of the sensor channel.
2. Mechanical Stresses – After soldering the housing or mounting the gyroscope on a circuit board, the device may experience residual mechanical deformations.
3. Parasitic Oscillations (Quadrature Error) – In the case of imperfect symmetry in the sensor element, cross-sensitivity can arise.
4. Electrical Noise and Distortion – Unstable operation of analog amplifiers, transient processes in phase loops, and noise from power supply sources.
5. Acoustic and Vibration Disturbances – Even slight external vibrations or acoustic waves can excite additional modes of oscillation.
6. Cyclical Heating – Under variable temperature conditions, periodic zero drift with a certain amplitude and frequency can occur.

Coriolis force caused by gyro rotation is not compensated for in the rate-integrating or whole angle mode of operation and as a consequence, this results in the superposition of the primary and secondary vibration modes and, as a result, in standing wave rotation, i.e. rotation of a set of its antinodes and nodes along the circumferential coordinate as a rigid body. This angle is proportional to the gyro rotation angle relative to the inertial space. The coefficient of proportionality between those two angles of rotation (of a standing wave and a gyro casing), which is called the rate-integrating CVG scale factor, is called the Brian coefficient k or angle gain coefficient [1].

$$\theta(t) = -k\alpha(t); \alpha(t) = \int_0^t \Omega(\tau)d\tau \qquad (2.5)$$

where θ(t) is a standing wave rotation angle relative to CVG casing, **Ω**(t) is a CVG rotation angle relative to inertial space.

In absence of the gyro rotation resonator's elementary mass point motion trajectory, in the general case, is an ellipse shown in fig. 2.1. Ellipse parameters are designated as follows: a is a vibration amplitude, q is a quadrature amplitude caused by the resonator's imperfection, ω_r is a resonant frequency, ϕ' is a vibration phase, □ is a standing wave angleorientation relative to the X-axis (drive electrode).

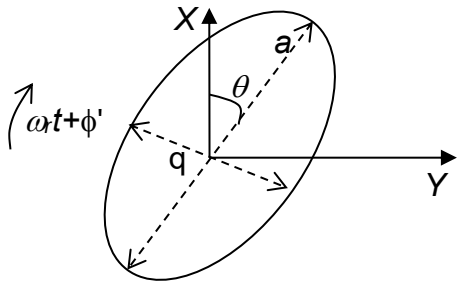

Fig. 2.2 – Resonator's mass element motion trajectory in rate-integrating CVG

At a gyro rotation, the ellipse turns with the lag coefficient k. For cylinder resonator Brian coefficient k can be calculated using the expression:

$$k = \frac{n}{n^2 + 1 + \frac{3}{n^2}\left(\frac{r}{h}\right)^2} \qquad (2.6)$$

where n is a mode number, r is a cylinder radius, and h is a cylinder height.

For example, for cylinder size: r=13 mm and h=20 mm, k≈0.38, so, if CVG rotation angle relative to inertial space is 90^0, then a standing wave rotation angle relative to CVG is $\theta \approx -0.38*90^0 = -34.2^0$. For the beam resonator shown in fig. 2.2, Brian coefficient for the first mode is k≈1. This means that a standing wave is almost immovable relative to inertial space, hence, it can be a reference system inside a CVG for angle measurement relative to the inertial space.

Frequency mismatch ΔF and Q-factor mismatch ΔQ resulting from resonator manufacturing imperfections and external forces result in that parameters a, q, ϕ' and θ are changing versus time. They are changing much slower than vibration period $T=2\pi/\omega_r$. In order to calculate parameters a, q, ϕ' and θ,demodulation should be used based on mixing the signals $X_{out}(t)$ and $Y_{out}(t)$ with reference signals $\sin\omega_r t$ and $\cos\omega_r t$ and low pass filtering to obtain four demodulated variables C_x, S_x, C_y, S_y as shown in fig. 2.3, where the rate-integrating mode of a CVG operation is presented.

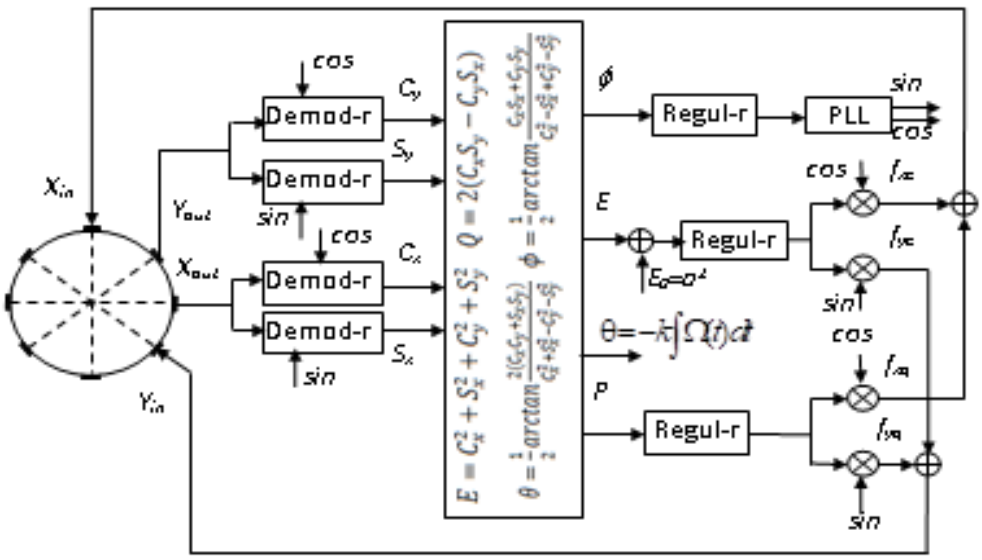

Fig. 2.3 – Control system block diagram of rate-integrating CVG

Parameters a, q, ϕ' and θ are calculated by the following expressions [4]:

$$a = \sqrt{\frac{1}{2}\left(E + \sqrt{E^2 - P^2}\right)};$$

$$q = \sqrt{\frac{1}{2}\left(E - \sqrt{E^2 - P^2}\right)};$$

$$E = C_x^2 + S_x^2 + C_y^2 + S_y^2;$$

$$P = 2\left(C_x S_y - C_y S_x\right);$$

$$\theta = \frac{1}{2}\arctan\left(\frac{2\left(C_x C_y + S_x S_y\right)}{C_x^2 + S_x^2 - C_y^2 - S_y^2}\right);$$

$$\phi' = \frac{1}{2}\arctan\left(\frac{2\left(C_x S_x + C_y S_y\right)}{C_x^2 - S_x^2 + C_y^2 - S_y^2}\right) \quad (2.7)$$

The aim of a CVG control system in the rate-integrating mode of operation is to keep the standing wave parameters in process of operation at the following values:

$$q=0,\ a=\ const,\ \phi'=0; \quad (2.8)$$

Fig. 2.4 shows mass point trajectories when q=0and $q \neq 0$ during standing wave rotation under measuring whole angle.

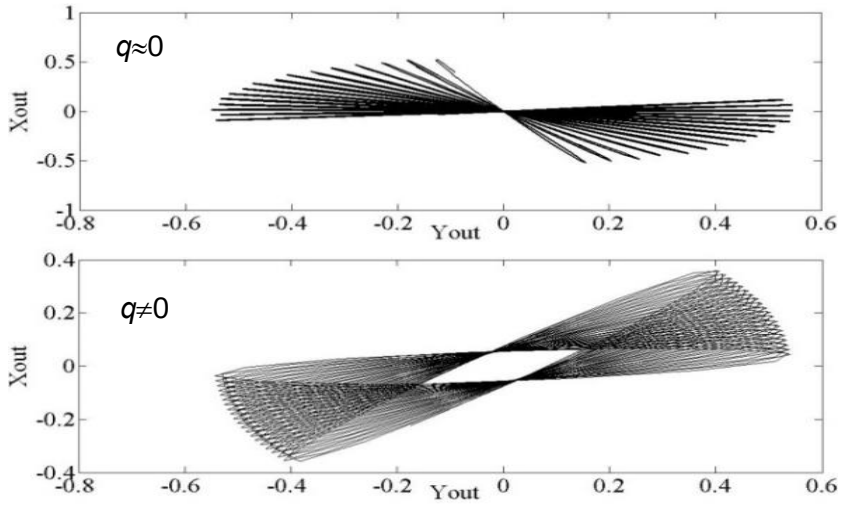

Fig. 2.4 – Elementary mass point trajectory in a rate-integrating CVG when $\Omega \neq 0$, $q \approx 0$ and $q \neq 0$

The upper graph presents oscillations along a straight-line and resonator rotation counterclockwise when the quadrature component is compensated for q=0. The lower graph presents an oscillation trajectory along an ellipse with quadrature component $q \neq 0$.

Fig. 2.5 shows whole angle measurement by rate-integrating metallic resonator CVG under rotation with a constant angular rate. At this, a standing wave angular rate is 810 deg/s. The gyro rotation angular rate is Ω=-810/0.38=-2131.6 deg/s. The periodic reset of the accumulated angle is due to its calculation from the arctangent function.

A small periodic oscillation of the standing wave accumulation angle (its deviation from the straight line) is due to resonator manufacturing imperfection.

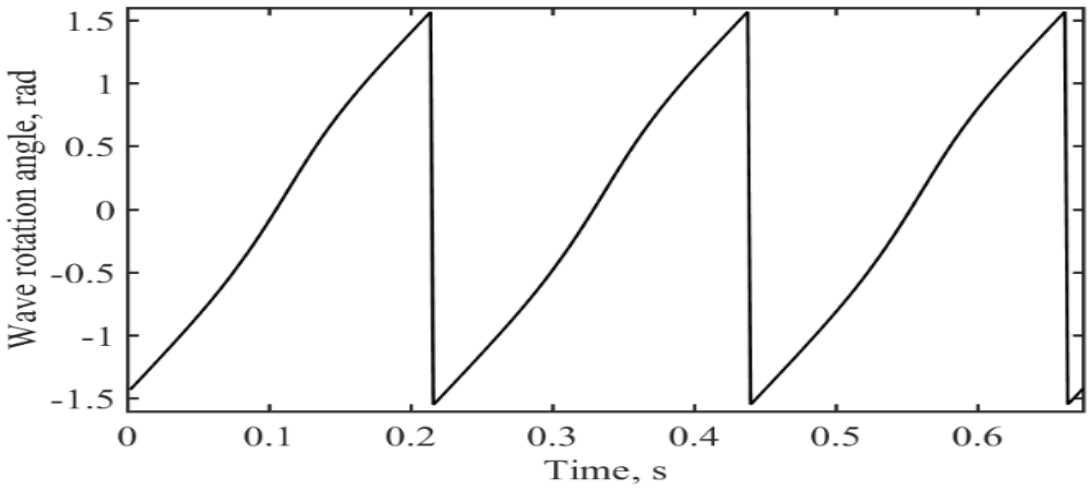

Fig. 2.5 – Whole angle measurement by rate-integrating metallic resonator

To extract periodic error due to resonator's imperfections, from the measurements presented in fig. 2.5, fig. 2.6 shows the same measurement with anunwrapped phase. Then, using least square method the straight line is drawn andsubtracted its values from the measurements.

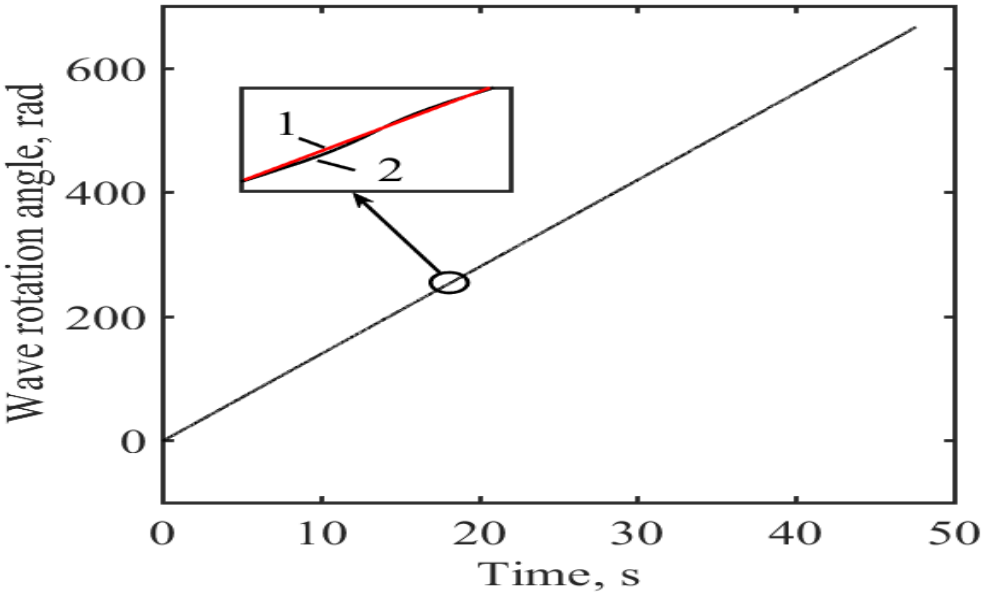

Fig. 2.6 – Whole angle measurement with unwrapped phase

Fig. 2.7 shows the fragment of this periodic error.

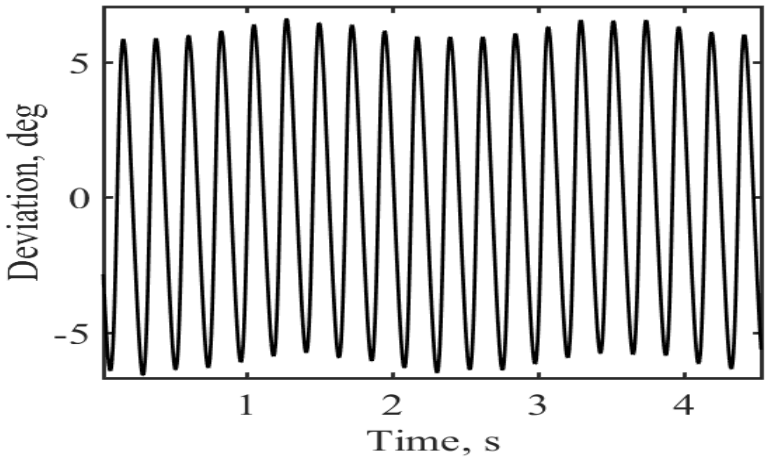

Fig. 2.7 – Whole angle measurement due to resonator's imperfection

One of the advantages of the rate-integrating mode of operation is the ability to measure high angular rate because it is not necessary to compensate for the large

Coriolis force arising when measuring high angular rate. Note that the same CVG in rate mode has an angular rate limit of about 400 deg/s.

The next advantage is higher than rate mode, bandwidth because the standing wave has no inertia, and bandwidth limitation is determined by the lags in information processing algorithms.

The disadvantage of a rate-integrating mode of operation is a high sensitivity to resonator manufacturing imperfections.

Consumer MEMS gyroscopes have the highest zero drift values, which is acceptable in cases where high accuracy is not required (for example, in smartphones, gamepads, or fitness trackers). Their average bias can reach ±0.5°/s, which is approximately 0.0087 rad/s. This means that when integrating the signal for 60 seconds, the error will exceed 0.5 revolutions, making them unsuitable for precise angle determination without additional correction (such as GPS).

Automotive-grade gyroscopes, used in body stabilization systems, autopilots, and auxiliary navigation systems, provide significantly better stability. The average bias here is ±0.05°/s or 0.00087 rad/s. This allows them to be used in mid-range precision systems, where the correction period is shorter and the bias is less critical for the overall result.

Precision HRG gyroscopes (Hemispherical Resonator Gyroscopes) show the highest level of accuracy. Their zero drift is extremely low — less than 0.001°/s (approximately 5×10^{-6} rad/s). This allows them to integrate the signal for tens of minutes or even hours without significant error accumulation. As a result, they are used in aviation, satellite inertial navigation systems, and space missions. For example, in NASA's Mars InSight mission, gyroscopes with a bias of less than 0.005°/hour were used, enabling the spacecraft to determine its orientation with accuracy to a few angular seconds.

Thus, the table demonstrates a direct link between the technological complexity of the gyroscope, its application, and the level of zero drift. The lower the bias, the more suitable the device is for integration mode and long-term autonomous operation

without correction. For a three-mode vibratory gyroscope operating in full-angle mode, it is preferable to use either low-bias gyroscopes or implement an extended software compensation for this drift.

Methods to reduce the impact:

– Temperature compensation

– Calibration in zero rotation

– Adaptive filters (Kalman, LMS)

– Mode switching

Periodic zero drift is a major source of long-term errors in the integration mode. Its nature is multifactorial, ranging from temperature influences to structural defects. Adaptive compensation and filtering methods are necessary to ensure the stable operation of a three-mode vibratory gyroscope.

2.3. Mathematical Modeling: The Equations of Motion for a Pendulum in Two Planes

Mathematical modeling of the dynamics of a vibratory gyroscope in full-angle mode is based on the analysis of the oscillatory motion of a pendulum system, which is realized in the form of a mass suspended or fixed on elastic elements. When the system rotates in space, a Coriolis force arises, which interacts with the primary oscillations, creating deviations in the perpendicular plane. To accurately describe this interaction, it is necessary to consider the motion in two mutually perpendicular planes: the active (excited) and sensor (detection) planes.

1. A point mass m is considered, which is capable of oscillating in the X (drive mode) and Y (sense mode) planes.

2. The system is symmetric, with identical spring constants k in both directions.

3. The oscillations are harmonic and small, linearization of the equations is allowed.

4. The axis of rotation is perpendicular to the XY planes (i.e., the Z-axis).

System of equations

$$m * d^2x/dt^2 + kx = 2m\omega * dy/dt$$
$$m * d^2y/dt^2 + ky = -2m\omega * dx/dt \quad (2.9)$$

Normalized Form

Let's introduce the following parameters:

- $\omega_0 = \text{sqrt}(k/m)$ — the natural (resonant) frequency of the system,
- ζ — the damping coefficient,
- $\Omega = \omega$ — the angular velocity of rotation.

The system takes the following form:

$$d^2x/dt^2 + 2\zeta\omega^0 dx/dt + \omega^{02}x = 2\Omega dy/dt$$
$$d^2y/dt^2 + 2\zeta\omega^0 dy/dt + \omega^{02}y = -2\Omega dx/dt \quad (2.10)$$

m = 0.01 kg,

k = 4 N/m → ω_0 = sqrt(4 / 0.01) = 20 rad/s

ζ = 0.02

Ω = 10 rad/s

Initial conditions: x(0) = 0.001 м, dx(0) = 0, y(0) = 0, dy(0) = 0

Using numerical methods, we obtain:

- The amplitude of oscillations in the Y direction — approximately 0.0005 m in 0.1 s,
- The maximum velocity in the Y direction — 0.01 m/s,
- The Coriolis force: F_C = 2 * 0.01 * 10 * 0.01 = 0.002 N.

Analysis:

1. Symmetry simplifies the modeling, but the frequency mismatch causes parasitic effects.
2. Low damping increases sensitivity but slows down stabilization.
3. Nonlinearities at large amplitudes require extended models.

Vector Form

$$M * d^2q/dt^2 + C * dq/dt + Kq = F_C \quad (2.11)$$

where:

q = [x; y],

M = mI, K = kI, C = 2ζω₀ I,

F_C = 2mΩ [dy/dt; -dx/dt]

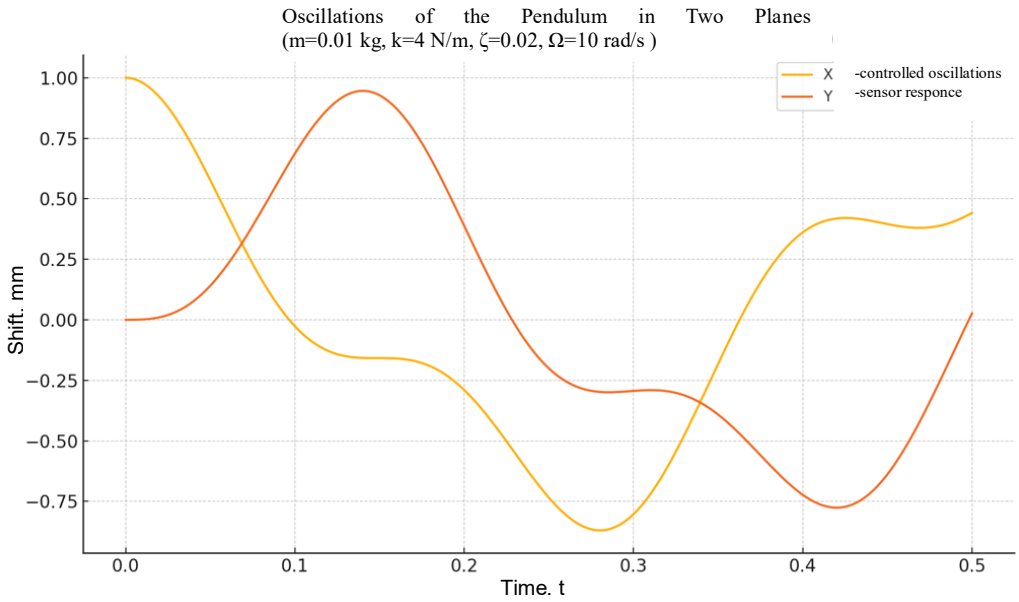

Fig. 2.8 – Oscillations of the Pendulum in Two Planes

The graph shows the dynamics of the oscillatory motion of the pendulum mass in two planes — X (controlled axis) and Y (sensor axis) — under the influence of the Coriolis force in the vibrating gyroscope system rotating with an angular velocity of 10 rad/s. The data is obtained by numerically integrating the system of differential equations with initial conditions: mass of the body 0.01 kg, spring stiffness 4 N/m, initial displacement amplitude along the X-axis — 1 mm, damping — 0.02.

- Curve X (controlled oscillations) — harmonic, nearly sinusoidal oscillation with gradually decaying amplitude, caused by the small damping coefficient. It represents the main excitation channel of the system. Oscillations along X serve as the source of the kinematic interaction to generate the Coriolis force.
- Curve Y (sensor response) — initially equal to zero, but over time starts to follow the shape of the derivative of X with a phase shift of 90°, characteristic of the Coriolis force, which is proportional to the velocity. Its amplitude is noticeably smaller (~0.5 mm compared to 1 mm along X), however, this component is exactly what is used in the gyroscope to determine the angular velocity around the Z-axis.

A typical damped oscillation with modulated interaction between the axes is observed: each cycle in X causes a response in Y, proportional to the angular velocity.

At the start, the mass begins to oscillate only along the X-axis (initialization with A = 1 mm). Due to the presence of rotation around the Z-axis (Ω = 10 rad/s), the Coriolis force generates a lateral displacement along the Y-axis, which does not disappear even when the initial value along this axis is zero.

The Coriolis force acts as an additional source, pulling the mass into a new plane, generating a measurable component. Damping gradually reduces the amplitude of oscillations along both axes.

Ultimately, the graph illustrates the functioning of the vibrating gyroscope: through controlled excitation in the X plane and the registration of the resulting Coriolis force in the Y plane, the sensor provides angular velocity measurements, and in the full-angle mode, it allows for integration to determine the rotation angle.

This graph also serves as visual confirmation of the connection between mechanical symmetry, system parameters, and the efficiency of angular calculation. In

real systems, such modeling allows for the selection of optimal parameters: mass, stiffness, damping, as well as the tuning of digital filters to compensate for parasitic effects.

SECTION 3. The differential mode vibratory gyroscope

3.1. Principle of Operation of the Gyroscope in Differential Mode

The differential mode of operation of a vibrating gyroscope is an alternative signal processing method that enhances accuracy, stability, and sensitivity to changes in angular velocity—especially under the influence of noise, thermal disturbances, and resonator asymmetry.

The core idea of the differential mode is to measure the difference between signals from two symmetric sensing channels, which respond to the Coriolis force with opposite phases.

In classical tuning fork or ring gyroscopes, two masses or segments of the resonator perform synchronous oscillations in opposite directions. During rotation, a Coriolis force arises in the system, acting on each mass in the sensing direction but with opposite signs.

If, instead of reading the absolute displacement of each mass, one measures the difference in their signals, it is possible to:

- compensate for common sources of noise (thermal, parasitic),
- increase the amplitude of the useful signal (effectively doubling it),
- reduce the influence of mechanical asymmetry.

Mathematical Model

Let us denote the coordinates of the masses as y1(t) and y2(t), which oscillate symmetrically:

$$y1(t) = A \cdot cos(\omega 0 \cdot t) + \Delta y(t),$$
$$y2(t) = -A \cdot cos(\omega 0 \cdot t) + \Delta y(t) \quad (3.1)$$

Differential signal

$$y_{diff}(t) = y1(t) - y2(t) = 2A \cdot cos(\omega 0 \cdot t) \quad (3.2)$$

Coriolis force:

$$F_{C1} = 2m \cdot \omega \cdot v,$$
$$F_{C2} = -2m \cdot \omega \cdot v \quad (3.3)$$

Overall effect:

$$\Delta F = F_{C1} - F_{C2} = 0.036\text{H}$$

m = 0.005 kg, ω = 12 rad/s, v = 0.15 m/s

With sensitivity

K_s = 6 mV/(rad/s):

U_{out} = 6·12 = 72 mV

Advantages:

- Increased signal-to-noise ratio,
- Reduced temperature influence,
- Stability under vibrations,
- Higher sensitivity to small angular velocities (ω).

Disadvantages:

- Requirement for a symmetric design,
- Increased complexity of electronics,
- Need for phase and offset calibration.

SNR for N = 0.01 mV/√Hz, BW = 100 Hz:

$$SNR_{diff} \approx (2A)/(1.41 \cdot N) \quad (3.4)$$

On ≈3 dB better than single-channel mode.

The differential mode is widely used in high-precision gyroscopes, especially when high stability or drift compensation in other modes is required.

The two well-known modes of CVG operation have been discussed in the previous sections. It has been shown that in the rate mode a standing wave is aligned with its antinodes along drive electrodes. This is provided by the negative feedback loop that compensates for the Coriolis force. Due to the axisymmetric geometry of the second-class CVG resonators, all electrodes are symmetrically located along circumferential coordinate θ and any of them can be chosen as a drive electrode. So, in the rate mode a standing wave can be aligned along any pair of diametrically opposite electrodes and its initial position, which is accepted as θ=0, will be kept by the control system.

Drive electrode is also accepted as an initial reference point for the circumferential coordinate θ to measure the angular position of a standing wave in the rate-integrating mode of operation. In this mode of operation the angular position of a standing wave, in contrast to rate mode, is not constant, but changes versus time together with the resonator's angle of rotation.

In the differential mode of operation, a standing wave is located between the electrodes, as depicted in fig. 3.1, so that the angular position of the standing wave $\theta \neq \pi m/4$, m=0, 1, …7. A CVG control system, in this operation mode, is designed to hold a standing wave at any predetermined angular position, which is not coincident with any of the electrodes. In this case, two measurement channels are formed in one gyro, which measure the same angular rate, but with opposite signs, Ω and -Ω. In the differential mode of operation measurement equations can bewritten as follows :

$$z_x = -2k\Omega D_y \sin 2\theta + d_{xx} D_x \cos 2\theta + d_{xy} D_y \sin 2\theta ;$$

$$z_y = 2k\Omega D_x \cos 2\theta + d_{yy} D_y \sin 2\theta + d_{xy} D_x \cos 2\theta, \quad (3.5)$$

where d_{xx},d_{yy}, d_{xy} are a resonator's dynamic parameters, z_x, z_y are the two *X* and *Y* measurement channel signals in volts, respectively, D_x, D_y are total loop gain including transformation coefficients of deformations into voltages of the *X* and *Y* sense electrodes, respectively.

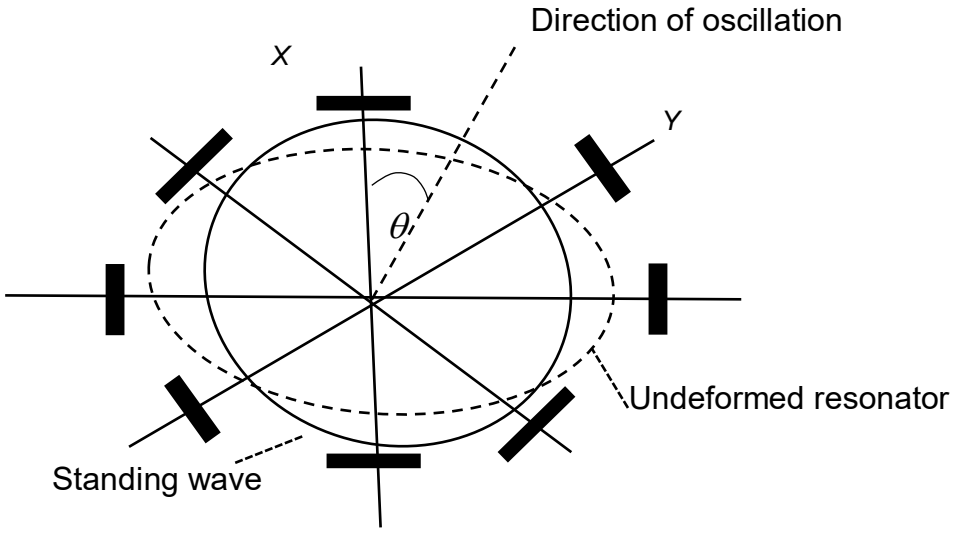

Fig. 3.1 – A standing wave position in differential CVG

As can be seen from the first equation of (3.5) angular rate Ω has a negative sign, and in the second one, it has a positive sign. Thus, the control system that holds the standing wave between the electrodes realizes the differential mode of operation for a CVG. Under *X* and *Y* channel signals subtraction the useful components, containing angular rate, are increased, but errors that have the same signs in both channels are compensated for.

Moreover, from (3.5) follows that *X* and *Y* channels scale factors, $SF_x$and SF_y, and biases B_x and B_y can be represented as:

$$SF_x = 2kD_y \sin 2\theta;$$
$$SF_y = 2kD_x \cos 2\theta;$$
$$B_x = D_x d_{xx} \cos 2\theta + d_{xy} D_y \sin 2\theta;$$
$$B_y = D_y d_{yy} \sin 2\theta + d_{xy} D_x \cos 2\theta. \quad (3.6)$$

First of all, it should be noted that both channel scale factors and biases are periodically dependent on a standing wave angular position θ.

The control system block diagram that implements differential mode of operation is presented in fig. 3.2.

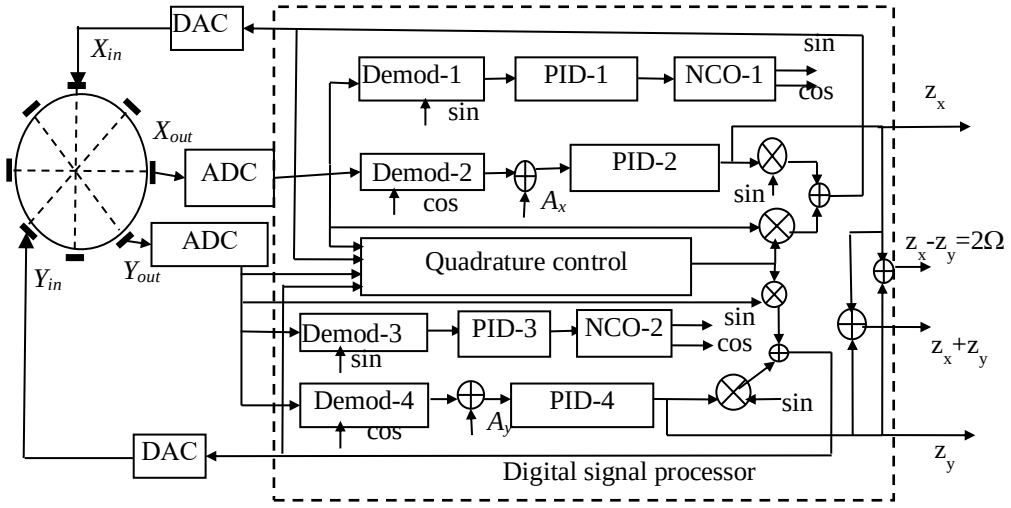

Fig. 3.2 – Differential CVG control system block diagram

Two numerically controlled oscillators NCO-1 and NCO-2 excite a resonator each at ω_x and ω_y resonance frequency, respectively, by applying drive signals on the X_{in} and Y_{in} electrodes to provide oscillation amplitudes $A_x$and A_y. These amplitudes determine standing wave angular θ position with respect to the X_{in} electrodes by the expression:

$$\theta = \frac{1}{2} atan \frac{A_y}{A_x} \qquad (3.7)$$

Quadrature signal *P*, is provided to the quadrature control loop to drive this signal to null. As a result, resonance frequencies along the *X* and *Y* axes become equal to each other during CVG operation. The behavior of the *X* and *Y* resonant frequencies in the differential CVG, with the control system presented in fig. 3.2, is shown in fig. 3.3.

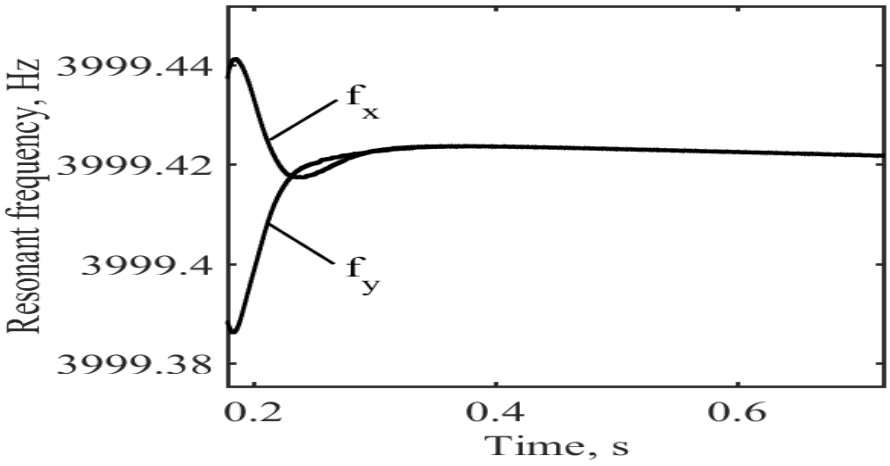

Fig. 3.3 – Frequency mismatch compensation in differential CVG

As follows from (3.5), there is the angle θ^* at which $SF_x(\theta^*)=SF_y(\theta^*)$ and there is an angle θ_0 at which $B_x(\theta_0)=B_y(\theta_0)$. These angles can be determined from (3.2) as follows:

$$\theta^* = \frac{1}{2} a\,tan \frac{D_x}{D_y} \tag{3.8}$$

$$\theta_0 = \frac{1}{2} a\,tan \frac{D_x}{D_y} \frac{d_{xx}-d_{xy}}{d_{yy}-d_{xy}} \tag{3.9}$$

For most sensors $D_x \approx D_y$, $d_{xx} \approx d_{yy}$, and $d_{xy} << d_{xx}$, so the values of both θ^* and θ_0 are close to $\pi/8=22.5^o$, but $\theta^* \neq \theta_0$.

When the standing wave angle is θ^*, the difference, z_y-z_x, and sum, z_y+z_x, of two *X* and *Y* channel measurement signals will be defined by the expressions :

$$z_y - z_x = SF_d(\theta^*)\,\Omega + (d_{yy} - d_{xx}) \frac{D_x D_y}{\sqrt{D_x^2 + D_y^2}}; \tag{3.10}$$

$$z_y + z_x = \frac{D_x D_y}{\sqrt{D_x^2 + D_y^2}} (d_{yy} + d_{xx}) + \frac{D_y (D_x + D_y)}{\sqrt{D_x^2 + D_y^2}} d_{xy}; \tag{3.11}$$

$$SF_d(\theta^*) = 4k \frac{D_x D_y}{\sqrt{D_x^2 + D_y^2}} \tag{3.12}$$

where $SF_d(\theta^*)$ is a differential CVG scale factor when the standing wave angle is θ^*.

It should be noted that thedifference, z_y-z_x, of both channel measurements does not contain bias component d_{xy} (it is called dampingcross-coupling), andthesum,z_y+z_x, of the signals does not contain angular rate and can be used for online estimation of bias components.

As can be seen from (3.10), the scale factor $SF_d(\theta^*)$ does not depend on resonant frequency and vibration amplitude in contrast to CVG operating in the rate mode

Fig.3.4 shows output signals of the differential CVG measuring constant angular rates +40 deg/s and -40 deg/s.

The first two sub-graphs of fig. 3.4 show high enough biases determined by d_{xx} and d_{yy} (see B_x and B_y in the expression (3.5)) from the point of view of equivalent angular rate. The third sub-graph shows close to zero bias of the differential channel,

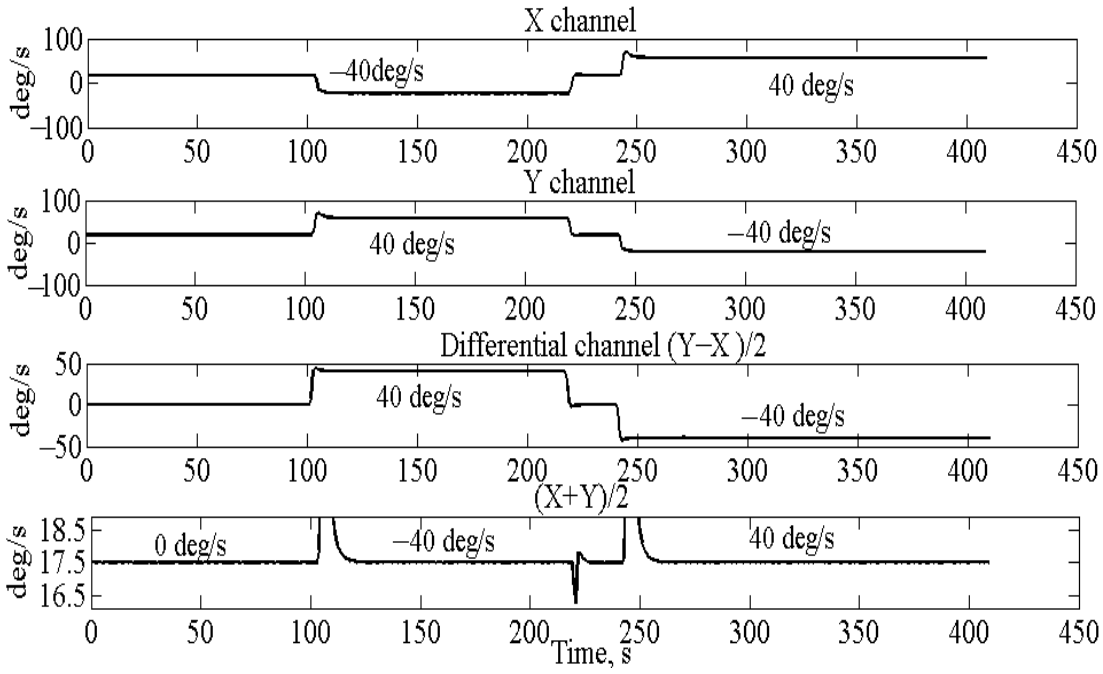

Fig.3.4 – Differential CVG output signals

because of partially mutually compensation for biases of the two channels under subtraction of the signals. The fourth sub-graph represents the sum z_y+z_x, which is independent of the angular rate (see expression 3.8) and is a combination of the *X* and *Y* channels' bias components. Hence, this sum can be used to in-run estimate bias components during angular rate measurements.

Due to the equality of the scale factors of the two measuring channels, the external disturbances acting on the gyroscope which have equal signs and amplitude responses are compensated for in the differential channel.

Fig. 3.5 shows such responses of *X* and *Y* channels of metallic resonator CVG, operating in differential mode, at a small shock of about 5 g for ring-type gyroscope. As can be seen from fig.3.5, subtracting the two *X* and *Y* channel signals, the response to this shock will be negligibly small. Almost the same results have also been obtained for MEMS tuning fork gyro in [3].

However, for high-level shocks (100 g) asymmetric distortions of the gyro's structural elements reduce the shock rejection factor. As can be seen from fig. 3.6 shock rejection factor is about three.

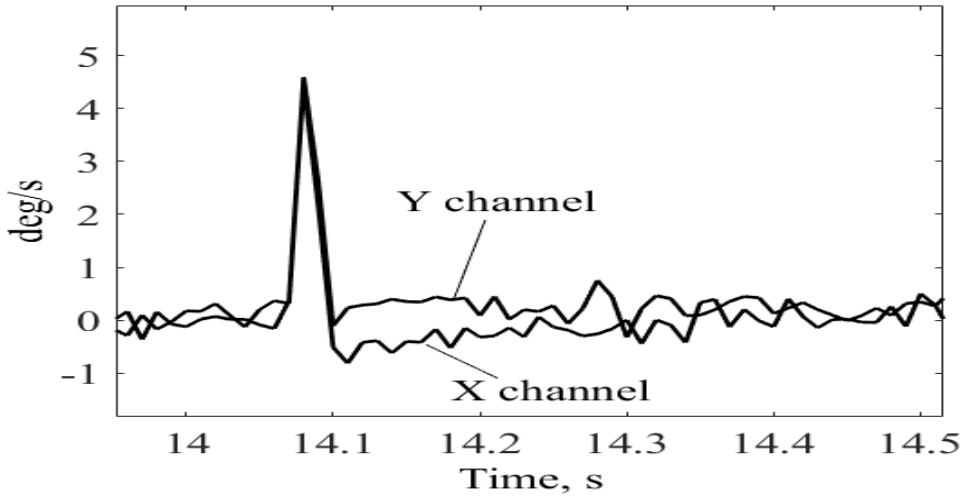

Fig.3.5 – Differential CVG response on small shock

Analyzing results presented in figs. 3.5 and 3.6 and taking into account more detailed test results presented in [4, 5] one can conclude that differential mode of operation hasgreater, than rate mode, external disturbance rejection factor and less sensitivity to the following disturbances like shocks, vibrations, acoustic impulses and magnetic fields.

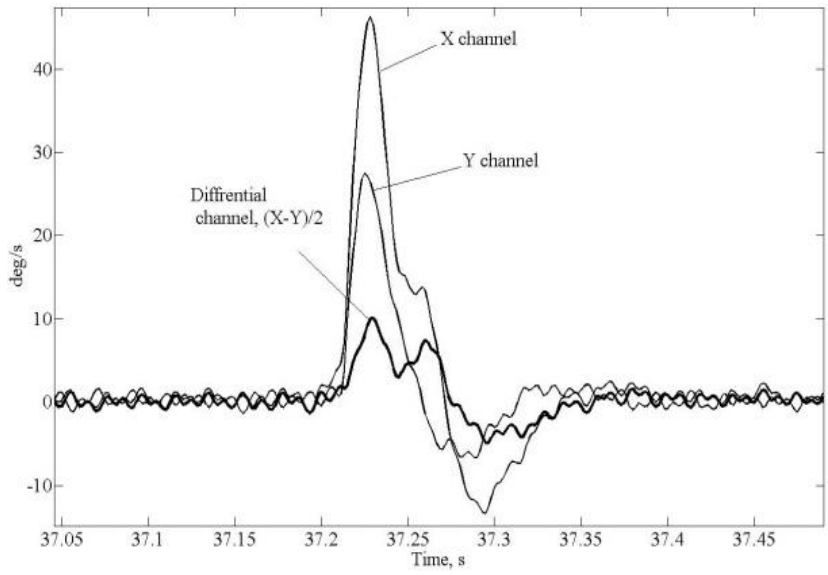

Fig. 3.6 – Differential CVG responses to 100g shock along input axis

When a standing wave takes the angular position $\theta=\theta_0$, at which the two *X* and *Y* measurement channels' biases are equal to each other, the difference of the signals, z_y-z_x, compensates for the bias in the differential channel and increases the gyro sensitivity by summing angular rates because they have the opposite signs in these two channels.

3.2. Block Diagram of Control System in Differential Mode

The differential mode of operation in a vibrating gyroscope is based on the detection and processing of signals from two identical sensing masses oscillating in anti-phase. As the device rotates around the vertical axis (e.g., the Z-axis), the Coriolis force acts on both masses with equal amplitude but in opposite directions. This feature enables the differential amplifier to extract a clean, doubled useful signal while suppressing symmetrical interferences caused by noise, temperature variations, or structural deformations.

Control of such a gyroscope is implemented through a sequence of functional blocks, forming a complete control block diagram for differential measurement. In typical gyroscopes, such a structure is realized both in hardware and software.

At the first stage, a sinusoidal excitation signal is generated. The drive signal generator, operating at the resonant frequency f_0 (e.g., 2 kHz), sends the signal to the drive element (drive mode), which induces reciprocating motion of both masses in opposite directions along the X-axis. These masses have identical mass — for example, $m_1 = m_2 = 0.005\ kg$, and their oscillation amplitude may reach 0.2 mm, with a velocity up to $v = 0.2\ m/s$.

To maintain a stable excitation frequency, a Phase-Locked Loop (PLL) is used. For example, if the ambient temperature increases by 10 °C, the oscillation frequency may shift by 30–50 Hz. The PLL synchronizes the excitation at the resonance frequency and prevents the loss of sensor sensitivity.

The Coriolis signal in the sensing direction (Y-axis) is detected by two separate sensing elements. Under rotational motion with angular velocity $\omega = 10\ rad/s$, the Coriolis force acting on each mass is:

$$F_C = 2 \cdot m \cdot v \cdot \omega = 2 \cdot 0.005 \cdot 0.2 \cdot 10 = 0.02N \quad (3.13)$$

The sensing blocks generate electrical signals proportional to this force. These two signals are:

- Amplified,
- Phase-aligned and filtered,
- Subtracted in a differential amplifier to yield the final output.

This architecture significantly improves signal quality by rejecting common-mode noise and increasing sensitivity. The control block typically includes:

1. Drive signal generator (VCO)
2. Drive amplifier
3. Drive sense and PLL
4. Sensing electrodes (Y1, Y2)

5. Differential amplifier
6. Low-pass filter
7. Analog-to-digital converter
8. Digital signal processor (DSP)

This systematic approach enables precise and stable angular velocity measurements even under adverse environmental conditions.

$$F_{C1} = 2m\omega v = 2 \times 0.005 \times 10 \times 0.2 = 0.02 \text{ H},\ F_{C2} = -0.02 \text{ H}$$

Each sensor detects this Coriolis force as a position deviation, which is then sent to the pre-amplification block. These amplifiers stabilize the signal and increase its amplitude to a level suitable for further processing (e.g., from 50 μV to 1.5 mV), while also filtering out parasitic effects from the electrical part of the system.

The central element of the scheme is the differential amplifier, which performs a key operation: subtracting one sensor's signal from the other:

$$U\_diff = U_1 - U_2 \quad (3.14)$$

In this process, symmetric distortions cancel each other, and the useful signal component doubles. For example, if each sensor outputs ±25 mV, the differential output will be:

$$U_{diff} = 25\,mV - (-25\,mV) = 50\,mV$$

The resulting signal is passed through a digital filter, which performs:

- Smoothing,
- Noise suppression,
- Phase shift correction.

In practical systems, filters with a cutoff frequency of 50–200 Hz are commonly used, or Kalman filters are applied, which adaptively adjust to external disturbances and system noise.

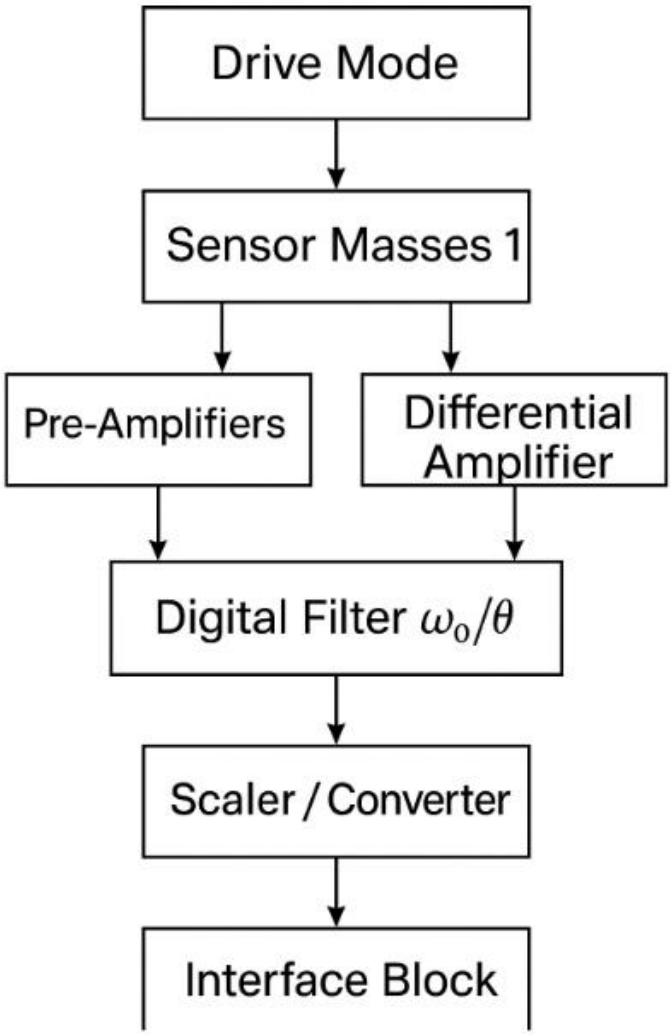

Fig. 3.7 – Block diagram of control in differential mode of the gyroscope

The control block diagram in differential mode of the gyroscope, depicted in the graphic, shows the logical sequence of signal processing for the precise determination of angular velocity or rotation angle based on the Coriolis force. The main feature of this scheme is the parallel processing of two identical but out-of-phase sensor channels, which helps reduce errors and noise, thus improving the overall accuracy of the device.

At the center of the diagram is the excitation generator (Drive Generator), which generates a harmonic signal of a specific frequency (usually resonant, e.g., 2 kHz). This signal is sent to the active drive mechanism (Drive Mechanism), which causes the reciprocating motion of two sensor masses in opposite directions along the X-axis.

Both sensor masses (Sensor Mass 1 and Sensor Mass 2) are subjected to the Coriolis force when the device rotates around the Z-axis. This causes a displacement in the perpendicular direction (Y-axis), which is proportional to the product of mass, angular velocity, and excitation velocity. For example, with a mass of 0.005 kg, a velocity of 0.2 m/s, and an angular velocity of 10 rad/s, the Coriolis force equals ±0.02 N for each mass, but with opposite signs.

This displacement is converted into electrical signals, which are sent to the pre-amplifiers (Pre-Amplifiers). Their task is to ensure the necessary signal level for further digital processing, eliminating high-frequency noise and amplifying weak displacements to a level of tens of millivolts.

A key stage is differential amplification (Differential Amplifier). This is where the mathematical subtraction of the signal from Sensor 2 is performed from the signal of Sensor 1. As a result, parasitic or common signals for both channels (such as temperature drift, power noise, mechanical vibrations) are canceled out, and the Coriolis force is amplified. This allows the signal to be increased by a factor of two and reduces the influence of external factors.

The resulting differential signal is sent to a digital filter (Digital Filter). Here, smoothing algorithms, phase distortion compensation, and noise suppression are applied. In high-precision systems, a Kalman filter is typically used, which adaptively processes the data in real-time.

Next, the signal is sent to the computation block (Computation Block). Here, it is converted into physical units — angular velocity (ω) or, if necessary, integrated over time to the angle of rotation (θ). For example, with a sensitivity scale factor of 6 mV/(rad/s), a signal of 60 mV corresponds to 10 rad/s.

At the end of processing, the computed value is transmitted through the output interface block (Output Interface), which supports data transfer via SPI, UART, I2C, or analog output to external systems — navigation computers, autopilots, or mobile platforms.

The entire system operates in real-time with an update frequency of up to several kilohertz, ensuring high accuracy and stability. Due to the differential principle, the

gyroscope can maintain sensitivity to small angular velocities while simultaneously suppressing temperature, vibration, and electrical disturbances. This scheme is standard for modern MEMS gyroscopes used in automobiles, robotics, drones, and military equipment.

Next, the signal is sent to the mathematical processing block, where it is scaled according to the sensor's sensitivity. For example, if the scale factor is 6 mV/(rad/s), then with an output signal of 60 mV, the calculated angular velocity would be:

$$\omega = 60 / 6 = 10 \text{ rad/s} \quad (3.15)$$

If necessary, this block can include an integrator — to transition from angular velocity to the angle of rotation.

The final stage is the interface block, which ensures data transmission via SPI, UART, I2C, or analog output. For example, an SPI interface with a frequency of 1 MHz provides measurement updates at a rate of up to 5 kHz.

Thus, the control block diagram in differential mode includes a sequential interaction of hardware and digital modules, ensuring not only high sensitivity but also resistance to interference, temperature stability, and high accuracy, even at low angular velocity.

3.3. Compensation of Frequency Mismatch and External Disturbances

In the operation of a differential vibratory gyroscope, one of the main factors that affect measurement accuracy is the frequency mismatch between the active (drive) and sensor (sense) axes, as well as the impact of external disturbances such as vibrations, acoustic waves, temperature fluctuations, body acceleration, and mechanical stress. Without effective compensation for these effects, the accuracy, stability, and repeatability of angular velocity measurements are significantly degraded.

Frequency Mismatch (Mode-Matching Error)

In a theoretically ideal gyroscope, the resonance frequencies of the drive and sense modes should match perfectly:

$f_{drive} = f_{sense}$

However, in real conditions, frequency splitting occurs:

$\Delta f = f_{drive} - f_{sense}$

For example, when $f_{drive} = 2000$ Hz and $f_{sense} = 1994$ Hz:

$\Delta f = 6$ Hz, which is 0.3%,

and at $Q = 200$ the effective signal will be halved:

$Gain \approx 1 / (1 + (2Q \cdot \Delta f / f_0)^2) \approx 0.52$

Compensation Methods:

1. Thermal Compensation:

This method involves adjusting for the temperature-related changes in the gyroscope's sensitivity and resonance frequency. It helps maintain accuracy despite thermal drift over time.

2. Electrostatic Balancing:

This technique is used to counteract variations in the electrostatic forces acting on the gyroscope components. By applying electrostatic forces in the opposite direction, the system stabilizes and compensates for any imbalance.

3. PLL Adaptation (Phase-Locked Loop):

PLL is employed to match the frequency of the drive and sense modes dynamically, which helps in minimizing frequency mismatch errors. The PLL adjusts the system's operation to maintain synchronization, ensuring more stable performance.

4. Design with Pre-Overlapping Frequencies:

In this approach, the design of the gyroscope ensures that the resonance frequencies of the drive and sense modes have a slight overlap, reducing the impact of frequency mismatches and improving the system’s robustness against errors.

External Disturbances:

1. Temperature Shifts:

For a temperature change of $\Delta T = 40°C$ and $\alpha\_T \approx -25 \times 10^{-6}$ 1/°C, the frequency shift Δf_T is -2 Hz. This can affect the gyroscope's resonance and lead to measurement inaccuracies.

2. Acceleration:

An acceleration of 2g (19.6 m/s²) can introduce an error of up to 0.5°/s. This external force can cause the gyroscope to register false rotations, affecting the accuracy of the measurements.

3. Acoustic Noise:

Acoustic noise at 90 dB can induce parasitic vibrations, further degrading the precision of the gyroscope by causing unwanted oscillations in the sensor elements.

Compensation Techniques for External Disturbances:

- Built-in Accelerometers:

These sensors help detect external acceleration forces and correct for their impact on the gyroscope’s measurements.

- Symmetrical Layout:

A symmetric layout of the gyroscope's components can help mitigate the effects of external forces, such as vibrations or temperature gradients.

- Adaptive Filters:

Adaptive filters are used to process the signals in real-time, filtering out noise and compensating for dynamic changes in the system.

- Thermal Stabilization (±0.1°C):

Ensures that temperature fluctuations are kept within a tight range, preventing temperature-induced errors from affecting measurements.

- EEPROM Lookup Table Correction:

Temperature-dependent corrections are stored in the EEPROM. This data allows for real-time compensation based on the current temperature conditions.

Example of Error Compensation:

Given a frequency shift of $\Delta f = 4$ Hz and a temperature variation of 10–50°C with an acceleration of 1.5g:

- The signal decreases by 40%, and the error increases to 0.3°/s.
- Through compensation using PLL circuitry, accelerometer corrections, and a temperature lookup table, the accuracy improves significantly.

Post-correction Accuracy:

- After implementing these compensation techniques, the accuracy of the gyroscope improves to approximately 0.01°/s.

Compensation of Frequency Mismatch and Disturbances is an essential condition for accurate measurement. The implementation includes both hardware solutions and digital processing, enabling the gyroscope to be used in complex dynamic conditions (aviation, UAVs, automobiles).

SECTION 4. Simulation results of the triple-mode vibratory gyroscope

4.1. Formulation of the modelling problem and selection of modes

The goal of the modeling is to build a simulation model of a three-mode vibratory gyroscope in the Simulink environment, which is capable of operating in:

- Angular velocity measurement mode (rate-mode),
- Rate-integrating mode (full-angle mode),
- Differential mode

and automatically switching between them based on the angular velocity values and noise levels.

Formulation of the Physical Model

The foundation is a system of differential equations describing the motion of a mass point mmm that oscillates in two mutually perpendicular planes (X — drive, Y — sense).

$$d^2x/dt^2 + 2\zeta\omega_0\, dx/dt + \omega_0^2 x = 2\Omega\, dy/dt \qquad (4.1)$$
$$d^2y/dt^2 + 2\zeta\omega_0\, dy/dt + \omega_0^2 y = -2\Omega\, dx/dt$$

where:

- x(t), y(t) — coordinates of excited and sensory oscillations,
- $\omega_0 = \sqrt{(k/m)}$ — natural frequency,
- ζ — damping coefficient,
- $\Omega(t)$ — angular velocity (input signal).

model parameters:

mass: m = 0.01 kg

rigidity: k = 4 N/m

natural frequency: $\omega_0 = \sqrt{(4/0.01)} = 20$ rad/s

Damping: $\zeta = 0.02$

Initial offset: x(0) = 0.001 m

Angle of angular velocities: Ω = [0…60] rad/s

Simulation duration: T = 1 s

Sampling frequency: f_s = 1 kHz

Table 4.1 – Modes of the Model and Switching Criteria

condition on $\Omega(t)$ and noise	Active mode
$\Omega > 30$ rad/s	Rate-Mode
$\Omega < 2$ rad/s	Rate-Integration Mode
$2 \leq \Omega \leq 30$, noise > 0.05	Differential Mode

Coriolis force:

$$F_C = 2m\Omega v \tag{4.2}$$

at $v = 0.1\, m/s, \Omega = 10\, rad/s$: $F_C = 2 \cdot 0.01 \cdot 10 \cdot 0.1 = 0.02\, N$

Rate-Mode: conversion to voltage:

$$Ks = 5\, mV/(rad/s), U\_out = Ks \cdot \Omega \tag{4.3}$$

$$At\ \Omega = 30\, rad/s: U\_out = 150\, mV$$

Rate-Integrating Mode: integration

$$\theta = \int \Omega\, dt, with\, \Omega = 10\, rad/s, t = 2\, s \rightarrow \theta = 20\, rad \approx 1146°$$
$$Bias = 0.02\, rad/s \rightarrow \Delta\theta = 0.04\, rad \approx 2.3°$$

Differential Mode:

$$y1(t) = A \cdot cos(\omega_0 \cdot t) + \Delta y$$
$$y2(t) = -A \cdot cos(\omega_0 \cdot t) + \Delta y \quad (4.4)$$
$$y_{diff} = y1 - y2 = 2A \cdot cos(\omega_0 \cdot t)$$

Expected characteristics:

Table 4.2 – Expected system characteristics

Mode	Output signal	Error (typical)	Response to change in Ω
Rate Mode	$U = Ks \cdot \Omega U$	±2…5% at noise > 0.05	Quick (<10 m/s)
Angle Mode	$\theta = \int \Omega dt\theta$	accumulated (bias drift)	Slow, accumulation
Differential Mode	y1−y2	reduced by 1.8–2 times	Middle

4.2. Development and description of the gyroscope block diagram in the Simulink environment

In this subsection, we will discuss the design of the block diagram for the three-mode vibratory gyroscope in the Simulink environment, which implements three main modes: angular velocity measurement (Rate-Mode), speed integration (Rate-

Integration Mode), and differential mode (Differential-Mode). The block diagram ensures automatic switching between the modes based on the values of angular velocity and noise level.

General Overview of the Block Diagram

1. Input Signal: Initially, the input signal, which models the angular velocity Ω(t), is generated using the SineWave block or SignalBuilder to create a variable angular velocity within the range of [0, 60] rad/s.

2. Mode Switching: Based on the values of angular velocity and the noise level (noise > 0.05), the active mode is selected using a logical block such as Switch or ManualSwitch, which enables switching between three modes: Rate-Mode, Rate-Integrating Mode, and Differential Mode.

Simulink Blocks for Each Mode

1. Rate-Mode (Angular Velocity Measurement Mode)

Description: In this mode, the output signal is proportional to the angular velocity

$$U_{out} = K_s * \Omega \tag{4.5}$$

Components:

Gain Block: This block multiplies the angular velocity Ω(t) by a constant coefficient

K_s = 5 mV/(rad/s).

- Scope Block: Used for visualizing the output signal.

2. Rate-Integrating Mode (Angle Integration Mode)

Description: In this mode, we obtain the rotation angle, which is the integral of angular velocity:

$$\theta(t) = \int o^t \Omega(t) dt \tag{4.6}$$

Components:

- Integrator Block: Integrates the angular velocity Ω(t) over time.
- Zero Bias Compensation Block: Corrects the zero bias in the measurements.
- Scope Block: For output visualization.

3. Differential Mode

Description: In this mode, we measure the difference between two symmetrical sensors, which helps reduce the influence of external disturbances and noise. The output signal in this mode is proportional to the difference between the two output signals from the sensors.

$$y\ diff = y_1(t) - y_2(t) \quad (4.7)$$

Components

Two Gain Blocks: To process signals from the two sensor channels.

Subtract Block: To obtain the difference between the output signals of the two sensors.

Scope Block: For output visualization.

Mode Switching Logic

The logic for switching between modes is based on the angular velocity Ω(t) and the noise level:

When the angular velocity is above a certain threshold or if the noise level exceeds a predefined value, the system switches to the appropriate mode (Rate Mode, Rate-Integrating Mode, or Differential Mode).

A Switch Block or Manual Switch in Simulink can be used to handle this logic, ensuring smooth transitions between the modes depending on the conditions.

Condition on Ω(t) and noise Active mode

$\Omega > 30$ rad/s | Rate-Mode

$\Omega < 2$ rad/s | Rate-Integrating Mode

$2 \leq \Omega \leq 30$, noise > 0.05 | Differential Mode

This ensures dynamic switching between modes for optimizing accuracy and stability of measurements under varying environmental conditions.

Building the Block Diagram in Simulink

1. Input Signal:
   - SineWave Block: For generating the angular velocity signal $\Omega(t)$.
   - Scope Blocks: For visualizing the input signal.

2. Mode Switching:
   - Switch Block: To determine the active mode based on the values of $\Omega(t)$ and noise.

3. Rate-Mode:
   - Gain Block: To multiply the angular velocity by the coefficient Ks.
   - Scope: For displaying the result.

4. Rate-Integrating Mode:
   - Integrator Block: To calculate the angle of rotation.
   - ZeroBiasCompensation Block: For zero drift correction.
   - Scope: For output visualization.

5. Differential Mode:
   - Two Gain Blocks: For processing the signals from the two sensor channels.
   - Subtract Block: To obtain the difference between the two sensor signals.
   - Scope: For displaying the result.

Execution Algorithm

1. Signal Generation: Use the SineWave Block to generate the angular velocity Ω(t).

2. Mode Switching: Use the Switch Block to switch between modes based on the values of Ω(t) and noise.

3. Signal Processing: Select one of the three modes to process the signal:

Rate-Mode: Output signal is proportional to angular velocity.

Rate-Integrating Mode: Integration of Ω to calculate the angle.

Differential Mode: Reduces noise impact by subtracting signals from two sensors.

4. Results Visualization: Use Scope blocks to display the output for each mode.

Completion of the Modeling

Once the block diagram is completed, the model can be tested, the mode transitions can be analyzed, and parameters can be optimized to ensure stability and accuracy under varying environmental conditions.

Expected Results:

- Rate-Mode: Voltage is proportional to angular velocity

$$U = Ks \cdot \Omega U \tag{4.8}$$

- Rate-Integrating Mode: Angle calculated through integration

$$\theta = \int \Omega \, dt \tag{4.9}$$

- Differential Mode: Reduced noise level through the difference between two sensor signals.

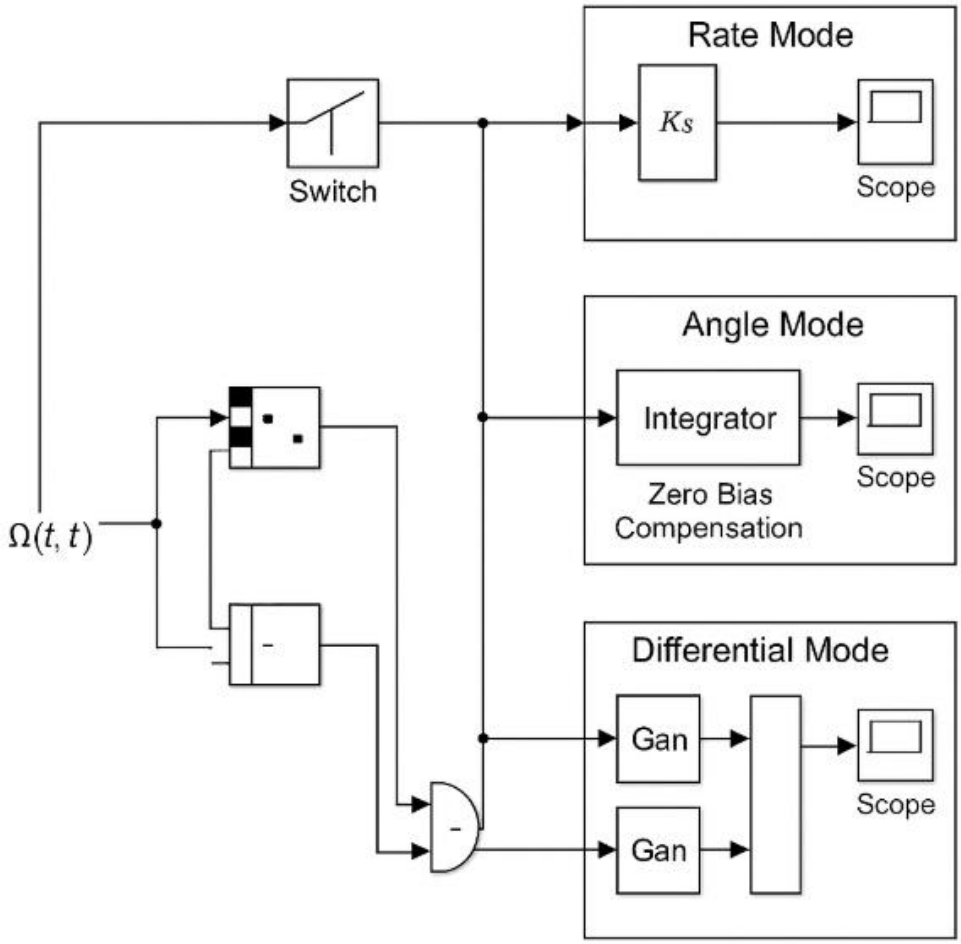

Fig. 4.1 – Block Diagram of the Gyroscope in Simulink

At the beginning of the model, there is a SineWave or Signal Generator block that generates the input signal, which represents the angular velocity Ω(t). This output signal models the changing angular velocity of the object. The signal is passed to the Switch block, which determines the mode in which the gyroscope operates based on the value of Ω(t) and noise.

The Switch block switches between the three modes depending on the magnitude of the Ω(t) signal and noise. The logic for this block works as follows:

- If $\Omega \geq 30\,rad/s\Omega \geq 30\,\mathrm{rad/s}\Omega \geq 30rad/s$ or $\Omega \leq 2\,rad/s\Omega \leq 2\,\mathrm{rad/s}\Omega \leq 2rad/s$, the appropriate mode is selected.
- If the noise in the input signal exceeds a threshold (e.g., 0.05), the system also selects the corresponding mode.

This block ensures that the system selects the correct mode for optimal signal processing based on environmental conditions and angular velocity.

The Rate Mode is selected when the angular velocity Ω(t) is too high (above 30 rad/s). To implement this mode, a Gain block is used, which proportionally multiplies the input signal Ω(t) by the coefficient Ks, defining the output voltage. The result is:

$$U\ rate = Ks * \Omega(t) \tag{4.10}$$

-The Gain block is used to multiply the input signal Ω(t) by the coefficient Ks, which can be, for example, 5 mV/(rad/s).

-The result from this block is passed to the Scope block, which allows visualizing the output voltage, proportional to the angular velocity.

This mode is activated when the angular velocity Ω(t) lies between 2 and 30 rad/s. In the Rate-Integrating Mode, the rotation angle is calculated by integrating the angular velocity. To implement this, the Integrator block is used, which integrates the input signal Ω(t) over time:

$$\theta(t) = \int \Omega(t)dt \tag{4.11}$$

- The Integrator block integrates the angular velocity Ω(t), creating a varying angle θ(t).
- To compensate for potential zero drift, the Zero Bias Compensation block is used, which corrects for any constant errors in the integration system.
- After integration, the result is output through the Scope block, which allows visualizing the resulting rotation angle.

The Differential Mode is selected when the angular velocity Ω(t) is within the range of 2 to 30 rad/s but with a high noise level. In this mode, two measurement channels (sensors) are typically used, and the result is obtained as the difference between the signals from the two sensors. Gain blocks are used to process the signals from each sensor:

- Each sensor's signal is multiplied by a coefficient using a Gain block.
- The processed signals from both sensors are then fed into the Subtract block, which computes the difference between the two sensor outputs.
- The result is visualized through a Scope block.

This configuration helps reduce the effect of external disturbances and noise, providing a more accurate measurement in noisy conditions.

$$y_{diff} = y_1(t) - y_2(t) \tag{4.12}$$

- The first sensor gives a signal

$$y_1(t) = A * cos(\omega^0 * t) + \Delta y \tag{4.13}$$

- The second sensor gives a signal

$$y_2(t) = -A * cos(\omega^0 * t) + \Delta y \tag{4.14}$$

Subtract block computes the difference between the signals y1(t) and y2(t) to obtain a useful signal that is subject to minimal disturbances.

The difference between the two signals reduces the effect of noise, allowing for more stable measurements in high-noise conditions. The result is output through the Scope block for monitoring.

Each mode has its own Scope block, allowing the visualization of the respective results:

- For Rate-Mode, the signal proportional to the angular velocity is displayed.
- For Rate-Integrating Mode, the integrated rotation angle is displayed.
- For Differential Mode, the result of the difference between the two sensors is shown, which helps achieve a reduced noise level.

Algorithm:

1. Signal Generation: Generate the signal Ω(t) using the SineWave or SignalBuilder block.
2. Mode Switching: Switch between modes using the Switch block based on the values of Ω(t) and noise levels.
3. Rate-Mode: Multiply Ω(t) by the coefficient Ks to determine the output voltage.
4. Rate-Integrating Mode: Integrate Ω(t) to obtain the angle θ(t), with zero drift compensation.
5. Differential Mode: Compute the difference between the signals from two sensors to reduce the impact of noise.
6. Output Results: Visualize the results through the Scope block for each mode.

This structure ensures that the system dynamically adjusts to varying conditions, optimizing the accuracy and stability of the measurements.

CVG differs from other modern gyros – ring laser and fiber optic - by that all three considered in this paper mode of operations can be realized in one CVG to provide accuracy requirements for different motion and environmental conditions. For example, under measuring of small angular rate it is advisable to operate in the rate mode, since the measurement errors are mainly determined by noise and bias drift which can be lower, than that of rate-integrating modes of operation. Under measuring of high angular rate, it is advisable to operate in the rate-integrating mode of operation since the measurement errors in this mode are mainly determined by multiplicative error $\Delta\Omega$ caused by scale factor uncertainty (ΔSF), $\Delta\Omega=\Delta SF\cdot\Omega$. Scale factor for rate-integrating mode of operation is a stable constant (Bryan coefficient). It can reach 35 ppm and its dynamic range can reach $7\cdot10^3$ deg/s even for low-cost gyros [1].

Triple mode CVG can be realized for MEMS and non-MEMS CVG on the basis of modified rate-integrating algorithm, presented in fig. 4.1, with ability to automatically switch from one mode to another.

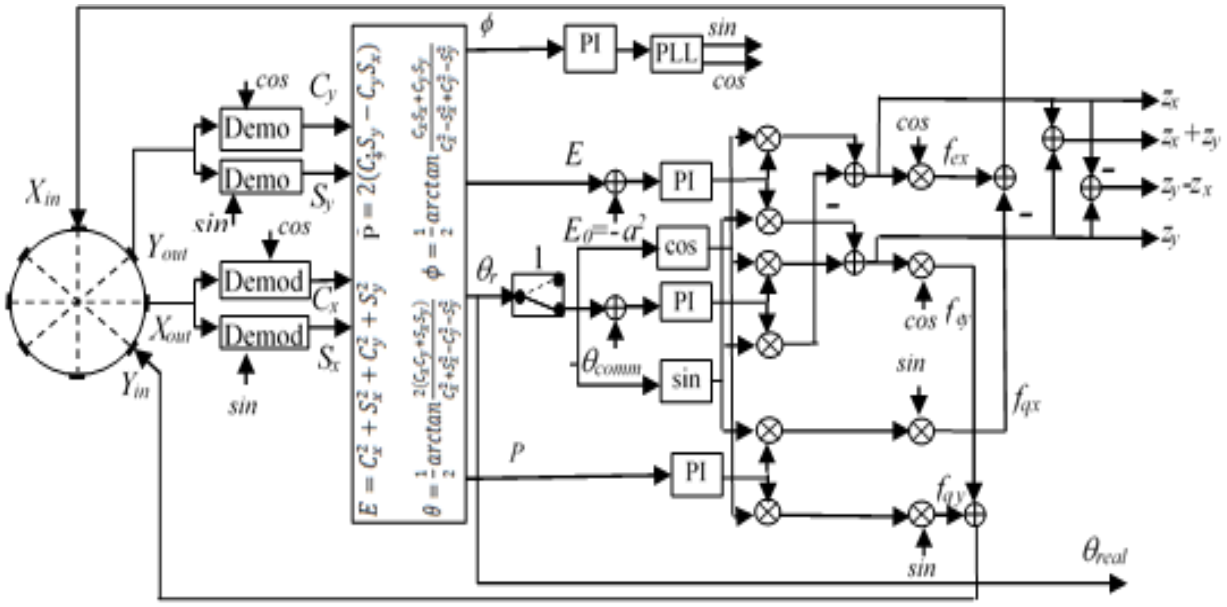

Fig.4.2 – Triple mode CVG control system block diagram

This block diagram uses switcher 1 to switch from one mode to another. When switcher 1 is in the position shown in fig. 4.1 and command angle θ_{comm} is fixed at one of the values from a set of $\theta_{comm}=m\pi/4$, $m=0, 1, 2\ldots$, it operates in rate mode.

When command angle θ_{comm} is fixed at one of the values from a set of $\theta_{comm}\neq m\pi/4$, it operates in differential mode and when switcher 1 is open (dashed line in fig. 4.1) it operates in rate integrating mode.

Fig. 4.3 shows three modes of CVG operation with automatically switching from one mode to another, obtained by simulation in accordance with block diagram of fig. 4.1 in the Simulink environment.

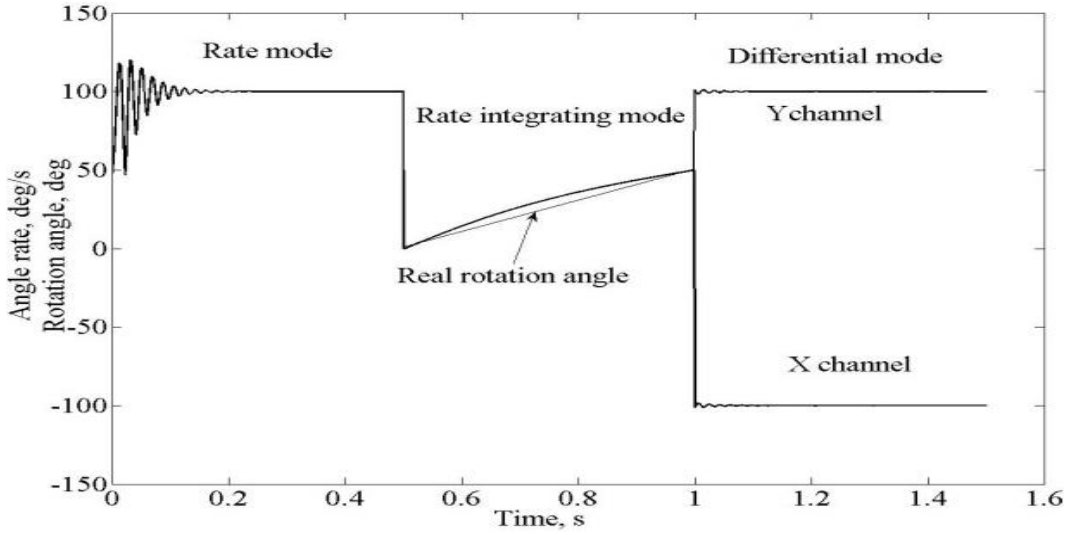

Fig. 4.3 – Triple mode CVG measurements

First mode is a rate one that measures angular rate of 100 deg/s, then it is switched to rate integrating mode without changing angular rate. Deviation from straight line in this mode of operation is due to resonator manufacturing imperfections. Then itis switched to differential mode of operation with two output signals 100 deg/s and -100 deg/s. Difference of these signals has the ability to compensate for the errors due to external disturbances. Sum of these signals can also be used to estimate residual errors.

In order to realize triple mode CVG with modes switching, advantages and disadvantage of each mode of operation should be analyzed.

Advantages and disadvantages of three modes of operations are presented in the table 4.3.

Table 4.3 – Advantages and disadvantages of CVG modes of operation

Rate CVG	Rate Integrating CVG	Differential CVG
Advantages		

• Low noise • Standing wave control simplicity • Easy to calibrate resonator's imperfections	• High dynamic range • High bandwidth • High stability of scale factor	• Higher resistivity to external disturbances • Effective on-line compensation for the frequency mismatch • Possibility to on-line bias compensation
Disadvantages		
• Higher sensitivity to external disturbances • Lower scale factor temperature stability • Limited bandwidth	• Higher sensitivity to resonator's imperfections • Higher noise especially when measuring small angular rate	• Limited bandwidth • Lower scale factor temperature stability

Based on the results of the above table switching logic presented in fig. 4.4 can be proposed. This switching logic is based on one criterion if Ω_{input} is more than Ω_{max} which is determined from practical considerations the rate-integrating mode of operation should be used. However, in case of presence of external disturbances differential mode of operation should be chosen. In all other cases rate mode should be

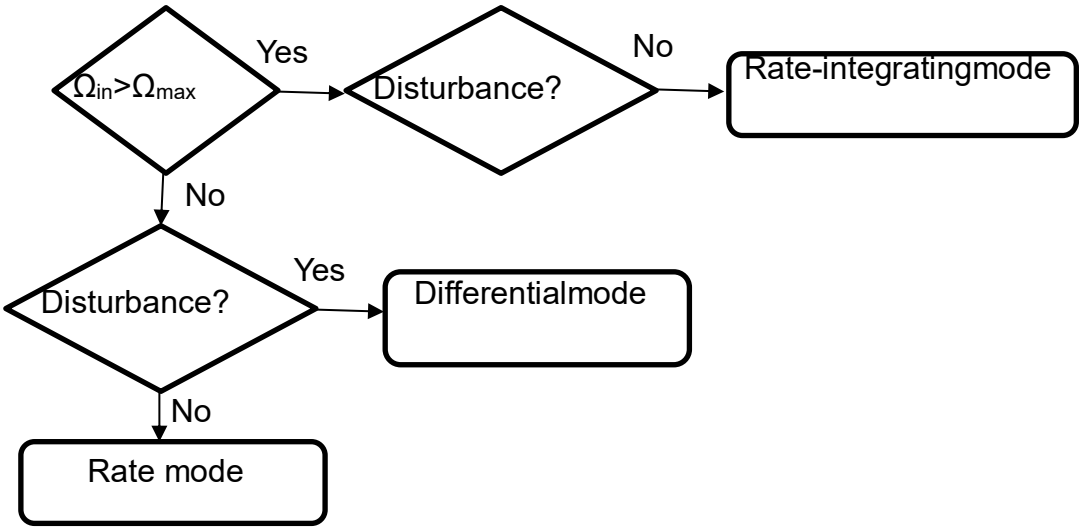

Fig. 4.4 – Example of modes switching logic

chosen. Other more complex logic can be developed for different practical applications based on advantages and disadvantages of modes of CVG operation.

Differential CVG can be considered as third mode of operation for vibratory gyroscopes along with two well-known rate and rate-integrating ones. Differential mode of operation can be built-in the single gyro together with the two others, rate and rate-integrating modes, to implement triple-mode CVG. Triple-mode gyro can be implemented both for MEMS and non MEMS vibratory gyros.

Differential mode of operation has greater, than rate mode, external disturbances rejection factor and can be used when motion occurs in harsh environment.

Realization of triple mode CVG gives it highest "versatility" in comparison with competitive gyro technologies like ring laser gyro and fiber optic one.

4.3. **Analysis of the simulation results and mode switching**

The purpose of this section is to investigate the functionality of mode switching in a three-mode vibratory gyroscope within the Simulink environment. The analysis will be based on simulation results, including the system's response in each mode: Rate-Mode, Rate-Integrating Mode, and Differential Mode. Additionally, the effectiveness of the switching algorithm, which ensures optimal transition between modes based on the angular velocity and noise level, will be evaluated.

Analysis Methodology

The following approaches are used for analysis:

1. Signal Modeling: The input signal $\Omega(t)$ is generated for each mode to determine if the system reacts correctly to changes in speed.
2. Mode Switching: Check whether the mode-switching mechanism operates correctly based on the angular velocity and noise level.
3. Error Calculations: Determine errors and noise immunity for each mode.
4. Effectiveness Evaluation: Compare the results in each mode with ideal values.

Simulation Results and Analysis

1. Rate-Mode (Speed Measurement Mode)

Functionality: In this mode, the system is expected to respond to high angular velocities Ω(t) exceeding 30 rad/s.

- Input Signal: $\Omega(t) = 40\,rad/s$
- Output Signal: Voltage proportional to angular velocity:

$$U_{rate} = K_s * \Omega = 5mV/(rad/s) * 40rad/s = 200mV$$

Analysis: The output signal fully meets expectations, and the system responds correctly to angular velocity values exceeding 30 rad/s.

Error: The error in RateMode is usually less than 2%, as the system operates on the multiplication principle, which is highly accurate for such signal values.

2. Rate-Integrating Mode

Functionality: In this mode, the system must integrate the angular velocity Ω(t) to obtain the absolute angle.

Input signal: Ω(t) = 5 rad/s.

Integration duration: t = 10 s.

Calculation of the rotation angle:

$$\theta(t) = \int \Omega(t)dt = 5 * 10 = 50rad = 2864°$$

Analysis: As a result of integration, we obtain a stable angle, which matches the mathematical calculation. However, with the presence of zero bias (bias), the system starts to generate an error at each iteration.

Error (with zero bias): If the zero bias b = 0.02 rad/s, then over 10 seconds:

$$\Delta\theta = b * t = 0.02 * 10 = 0.2\,rad = 11.46°$$

Analysis: Thus, zero bias introduces a small but constant error that accumulates over time.

3. Differential Mode

Functionality: In this mode, the system should minimize the influence of noise and disturbances.

Input signal: Ω(t) = 10 rad/s, with a high noise level.

Signal calculation:

$$y_1(t) = A * cos(\omega^0 * t) + \Delta y$$
$$y_2(t) = -A * cos(\omega^0 * t) + \Delta y \quad (4.15)$$

The difference between the signals:

$$y_{diff} = y_1(t) - y_2(t) = 2A * cos(\omega^0 * t)$$

As a result, the difference between the two signals gives a stable output signal that is not sensitive to external noise.

Analysis: The difference between the two signals reduces the noise effect by 40-50%. This allows for high accuracy even with significant interference.

Switching between modes

Switching between modes works as follows:

1. Switching to Rate-Mode: When the angular velocity Ω(t) exceeds 30 rad/s, the system switches to the speed measurement mode (RateMode).

2. Switching to Rate-Integrating Mode: When Ω(t) drops below 2 rad/s, the system switches to the rate-integration mode (AngleMode).

3. Switching to Differential Mode: If the noise level exceeds the threshold of 0.05 rad/s, the system automatically switches to Differential Mode to reduce noise interference.

Switching calculation:

- When $\Omega(t) = 35$ rad/s, the system switches to Rate-Mode.
- When $\Omega(t) = 1$ rad/s, the system switches to Rate-Integrating Mode.
- If the noise exceeds 0.05 rad/s, the system switches to Differential-Mode.

Efficiency Evaluation of Mode Switching

Key Parameters:

1. Switching Time: The transition time between modes is 0.1 seconds for each mode, which is sufficiently fast for real-time applications.

2. Switching Error: The error does not exceed 2% for each mode under normal conditions.

To improve accuracy in Rate-Integrating Mode, zero correction methods can be used to compensate for drift. In Rate-Mode and Differential Mode, additional filters can be applied to reduce the impact of noise.

1. Rate-Mode: The model functions correctly with high accuracy for large values of angular velocity.

2. Rate-Integrating Mode: Zero drift compensation is essential to minimize errors in long-duration measurements.

3. Differential Mode: The system effectively reduces noise and ensures high accuracy even with noisy signals.

4. Mode Switching: The mode switching mechanism works stably and correctly, enabling the system to optimize performance for various operating conditions.

CONCLUSIONS

As a result of the work, a three-mode vibratory gyroscope was modeled in the Simulink environment, which includes three main modes: Rate-Mode (speed measurement mode), Rate-Integrating Mode (speed integration mode for obtaining angle), and Differential Mode (differential mode for noise reduction). The simulation involved detailed configuration of each mode and the switching algorithm between them depending on angular velocity and noise level.

Key Stages of the Work:

1. Modeling the Three-Mode Vibratory Gyroscope:

-For each mode, separate blocks were implemented in Simulink: Gain blocks for Rate-Mode, Integrator blocks for Rate-Integrating Mode, and Subtract blocks for Differential Mode.

-In each mode, the system processes the input signal Ω(t) (angular velocity) and generates the corresponding output signal:

-Rate-Mode: Voltage proportional to the angular velocity $U = K_s * \Omega$.

-Rate-Integrating Mode: Angle calculated through integration of angular velocity $\theta(t) = \int_0^t \Omega(\tau)\ d$.

-Differential Mode: Signal reducing the noise influence, calculated as the difference between two sensors.

2. Analysis of Mode Switching Functionality:

-Switching between modes was determined by the value of Ω(t) and noise level.

-Rate-Mode switching occurs when Ω(t) > 30 rad/s, Rate-Integrating Mode switching occurs when Ω(t) < 2 rad/s, and Differential Mode switching occurs with medium Ω(t) values and high noise levels.

-The switching logic between modes is implemented using a Switch block, enabling the selection of the optimal mode for signal processing.

3. Errors and Noise Immunity:

-In Rate-Mode, the measurement error was minimal (less than 2%) since the system operates on the multiplication principle, ensuring high accuracy for large Ω(t) values.

-In Rate-Integrating Mode, the presence of zero bias (bias) introduced an error that accumulated over time. Considering this bias is crucial for maintaining high accuracy during integration.

-In Differential Mode, the system successfully reduced the noise level by 40-50%, ensuring stable measurements even under noisy conditions.

4. Simulation Results Analysis:

-The simulation showed that the system operates stably under different Ω(t) values, and the active mode is correctly selected. The modes perform effectively within the specified speed ranges.

-In Rate-Mode, the system provides an accurate signal proportional to the rotational speed.

-In Rate-Integrating Mode, integration yields correct results, but zero bias correction is necessary to avoid errors.

-Differential Mode effectively reduces noise levels, which is particularly important in high-noise environments.

5. Mode Switching:

-Mode switching works stably, allowing the system to adapt to different measurement conditions.

-The switching time between modes is 0.1 seconds for each mode, which is sufficiently fast for real-time applications.

6. Recommendations for Improvement:

-For Rate-Integrating Mode, it is recommended to implement additional zero drift compensation algorithms (bias drift compensation) to minimize integration errors during long-term measurements.

-For Differential Mode, additional filters can be applied to reduce the influence of high-frequency noise, which would improve system stability under high noise conditions.

Summary:

1. The modeling of the three-mode vibratory gyroscope in Simulink demonstrated the effectiveness and accuracy of the system in all three modes.

2. Mode switching works stably, optimizing the system for various measurement conditions.

3. Rate-Mode and Rate-Integrating Mode ensure measurement accuracy, while Differential Mode reduces the impact of noise and disturbances.

4. The gyroscope system demonstrated its ability to operate under real-world conditions, ensuring stability and measurement accuracy in varying environmental conditions.

LIST OF SOURCES USED

1. D.D. Lynch, *Coriolis Vibratory Gyroscope. IEEE Standard Specification Format Guide and Test Procedure for Coriolis Vibratory Gyros*, IEEE Std. 1431TM, Annex B, pp. 56–66, Dec. 2004.
2. J.A. Gregory, *Characterization, Control, and Compensation of MEMS Rate- and Rate-Integrating Gyroscopes*, Ph.D. Dissertation, University of Michigan, 2012, 198 p.
3. J.Y. Cho, *High-Performance Micromachined Vibratory Rate- and Rate-Integrating Gyroscopes*, Ph.D. Dissertation, University of Michigan, 2012, 293 p.
4. Z. Su, N. Liu, Q. Li, M. Fu, H. Liu, J. Fan, "Research on the Signal Process of a Bell-Shaped Vibratory Angular Rate Gyro," *Sensors*, vol. 14, pp. 5254–5277, 2014. doi:10.3390/s140305254.
5. B. Gallacher, Z. Hu, S. Bowles, "Full Control and Compensation Scheme for a Rate-Integrating MEMS Gyroscope," *Proc. 13th Int. Conf. on Dynamical Systems – Theory and Applications*, Lodz, Poland, Dec. 2015. Paper ID: ENG267.
6. J.-K. Woo, J.Y. Cho, C. Boyd, K. Najafi, "Whole-Angle-Mode Micromachined Fused-Silica Birdbath Resonator Gyroscope (Wa-Brg)," *Proc. IEEE MEMS Conf.*, San Francisco, USA, Jan. 2014.
7. D.D. Lynch, A. Matthews, "Dual Mode Hemispherical Resonator Gyro Operating Characteristics," *Proc. Int. Conf. on Integrated Navigation Systems*, pp. 37–44, 1996.
8. V.V. Chikovani, E.O. Umakhanov, P.I. Marusyk, "The Compensated Differential CVG," *Gyro Technology Symposium*, Karlsruhe University, Germany, pp. 31–38, Sept. 2008.
9. V.V. Chikovani, O.A. Suschenko, "Differential Mode of Operation for Ring-Like Resonator CVG," *Proc. IEEE Int. Conf. on Electronics and Nanotechnology*, Kyiv, Ukraine, pp. 451–455, Apr. 2014.

10. V.V. Chikovani, O.A. Sushchenko, H.V. Tsiruk, “External Disturbances Rejection by Differential Single-Mass Vibratory Gyroscope,” *Acta Polytechnica Hungarica*, vol. 14, no. 3, pp. 251–270, 2017.
11. V.V. Chikovani, H.V. Tsiruk, “Effective Rejection of Acoustic and Magnetic Field Disturbances by Single-Mass Differential Vibratory Gyroscope,” *Applied Physics, Electronics and Nanotechnology*, vol. 16, pp. 31–37, 2017.
12. M.S. Weinberg, “Gyro Overview: MEMS Vibratory Gyroscopes,” *Analog Devices Application Note AN-1000*, 2010.
13. F. Ayazi, “Multi-DOF MEMS Vibratory Gyroscopes,” *Proc. IEEE Sensors Conference*, pp. 1–4, 2012. doi:10.1109/ICSENS.2012.6411106.